AFCRL-68-0001

OBSERVATIONS OF STRATOSPHERIC CLEAR-AIR TURBULENCE AND MOUNTAIN WAVES OVER THE SIERRA NEVADA MOUNTAINS

An Analysis of the U-2 Flights of 13-14 May, 1964

by

Roger A. Helvey

James G. Edinger
Project Director

Department of Meteorology
University of California
Los Angeles, California 90024

AFCRL-68-0001

OBSERVATIONS OF STRATOSPHERIC CLEAR-AIR TURBULENCE AND
MOUNTAIN WAVES OVER THE SIERRA NEVADA MOUNTAINS

An Analysis of the U-2 Flights of 13-14 May, 1964

by

Roger A. Helvey

James G. Edinger
Project Director

Department of Meteorology
University of California
Los Angeles, California 90024

Contract No. AF 19(628)-4146

Project No.   8604
Task No.   860402
Work Unit No. 86040201

Meso-scale Circulations Project

FINAL REPORT

June 14, 1964 - September 14, 1966

December 1967

Contract Monitor: Samuel Penn
Meteorology Laboratory

Prepared for

AIR FORCE CAMBRIDGE RESEARCH LABORATORIES
OFFICE OF AEROSPACE RESEARCH
UNITED STATES AIR FORCE
BEDFORD, MASSACHUSETTS

ABSTRACT

Data obtained from a specially-instrumented U-2 aircraft have been used to relate clear-air turbulence with mountain wave structure, observed during two research flights in the stratosphere over the Sierra Nevada Mountains on 13 and 14 May, 1964. The several cases of severe turbulence encountered took place in regions immediately downstream of wave troughs, in areas of decreased static stability and slower wind speeds associated with the prevailing upwind tilt of the waves. An expression for the Richardson number is obtained which incorporates modifications imposed upon flow through stationary disturbances such as mountain waves.

I. INTRODUCTION

Awareness of high-altitude clear-air turbulence (HICAT) and a corresponding interest in the phenomena has been increasing in recent years as man extends his aerial activities throughout the upper troposphere and the stratosphere. Since mountain waves have been detected at stratospheric altitudes, investigation of their role in the production of HICAT is warranted.

Some of the high-altitude meteorological research flights made in spring 1964 for the Air Force Cambridge Laboratories (AFCRL) involved encounters with HICAT in the vicinity of mountainous terrain. The data was obtained by a specially instrumented U-2 aircraft operated by Electronic Systems Division of the U.S. Air Force Systems Command. The aircraft was based at Edwards Air Force Base in the Mojave Desert about 100 miles north of Los Angeles, California, and flown predominately in the upper troposphere and lower stratosphere, on various routes over the western United States. The data from these flights comprised part of that made available to UCLA, originally for study of diverse mesometeorological phenomena, but later narrowed specifically to investigation of HICAT.

Flight data from spring 1964 was surveyed in order to select interesting HICAT cases, since it was at this time that recording of an objective turbulence indicator became possible with addition of a vertical accelerometer to the U-2 instrumentation system. Of this series of flights, the two on the afternoons of 13 and 14 May, 1964 (designated ML-21 and ML-22, respectively) were found to be by far the best suited for analysis, due to the concurrence of three factors:

1) encounters with moderate to severe stratospheric CAT; 2) indications of mountain waves; and 3) well laid-out flight plans which would enable reconstruction of important aspects of the mountain wave structure.

II. FLIGHTS ML-21 and ML-22

1. Flight Plans

Approximate flight tracks for ML-21 and ML-22 are shown in Figure 1. Times are given in GCT. The flights originated at Edwards Air Force Base (EDW) shortly after noon and returned there the same afternoon local time, ML-21 on 13 may (2008 to 0145 GCT 13-14 May), and ML-22 on 14 May (2010 to 0040 GCT 14-15 May), 1964. Both included traverses over the Sierra Nevada Mountains at several levels in the stratosphere, as indicated schematically in Figure 2, between the VOR beacons near Friant (FRA), California on the west, and Tonopah (TPH), Nevada, on the east. The traverses have been numbered in the order flown. The traverse route lies along a line oriented approximately 245° -065° relative to true north, and crosses the Owens Valley a few miles north of Bishop (BIH), California, quite close to the general locale of the Sierra Wave Project operations conducted circa 1951-1955. This route is approximately perpendicular to the Sierra crest in this area, which is aligned at about 165° -345°. ML-21 had repeat traverses at the three lowest levels. Only one pass per level was flown for ML-22, but on this flight extensive horizontal areas were covered at 60,000 feet MSL north and south of the traverse line.

2. U-2 Data

The U-2 data used in this investigation were obtained from data books assembled by the university of Dayton, which reduces oscillograph records for AFCRL from the fast response U-2 instrumentation system. Flight ML-22 was investigated first. As initially made available to us, it had been reduced for mostly 5-second intervals, although portions were for 15 seconds. The plotting and smoothing was performed manually, which was tedious but led to detection and correction of some errors which might have otherwise gone unnoticed. Flight ML-21 was originally available as a mixture of 5-second and 32-second data. This flight was re-reduced at the University of Dayton according to our specifications, which were determined on the basis of our experience with ML-22. The final version provided a basic sampling interval of 10-seconds for the entire flight, with interesting portions of the traverse, and all soundings, read to 5-seconds. In addition, 2-second readings were made for the first and last several hundred feet of the soundings where they were most critical because of proximity to the traverse levels. Also, 60-second averages were obtained for certain data, and a set of supplementary coordinates with x-axis along the traverse route computed for that portion of the flight.

The parameters which we have utilized include:[*] Z_p (pressure-altitude in feet MSL), T (temperature in degrees C), Θ (potential temperature in

---

[*]Absolute heights above the terrain were available from an electronic altimeter. A study of this data was conducted for ML-21 in order to see if mesoscale variations in D-value could be detected. Detailed plots of pressure-altitude, underlying terrain altitude, radar-altitude, and derived D-values were made for portions of the ML-21 traverses over the Sierra crest. Although aircraft position over the terrain was determined carefully from the tracker camera photos and small scale topographic charts, the results were inconclusive because of scatter due to difficulty in properly matching radar altitudes with surface altitudes over the predominately rugged terrain.

degrees K), $\emptyset Z$ (ozone in μ mb), **WS** (wind speed in knots), **WD**(wind direction), and aircraft positions. Photographs looking downward and sideways were available from a 70 mm tracker camera which took 70-mm frames automatically throughout each flight at a rate of about two per minute. Vertical acceleration was measured by an accelerometer and used to indicate magnitude and duration of turbulence. The acceleration values were not tabulated; rather, the oscillograph was inspected at Dayton and apparently turbulent periods of flight and maximum acceleration noted. The winds and aircraft positions were derived from Doppler radar, and VOR check points. At times winds were not available when manuevers in turns and ascents/descents, or during turbulence, disrupted proper operation of the Doppler tracking system.

Because position inaccuracies sufficiently large to affect interpretation of the data were discovered during early stages of analysis, extensive usage was made of the tracker camera photos to obtain accurate position "fixes". For ML-21, these fixes were supplied to the University of Dayton for use in recomputation of aircraft positions, which have been used in this study. ML-22 position corrections were done by hand.

3. Weather Situation

Although a cold front passed through the region of interest during 13-14 May according to Weather Bureau analyses, it was weak and apparently produced little or no precipitation. An elongated surface low pressure area was present east of the Sierras, more pronounced on the first day. Winds aloft remained southwesterly

both days as shown by Figure 3. Isotachs and streamlines at three levels are drawn for 0000 GCT 14 and 15 May. On both days the flow is split into two major jets north and south of the Sierras at the highest levels, while at 700 mb several speed maxima appear, one downwind of the Sierras. A region of minimum speeds lies along the traverse route at 300 and 700 mb the first day, and on the second has moved somewhat south.

Figures 4 and 5 are vertical cross-sections of potential temperature (deg K), wind speed (knots), and direction, along the Pacific Coast at 0000 GCT on the two days. No major frontal zones are evident. Several jets appear near the upper tropopause. The tropospheric speed minimum over California has moved farther to the south on the second day.

The cross-sections were used to synthesize temperature and wind profiles upstream of the Sierras, as located by the vertical line between Oakland (OAK) and Point Arguello (PGU) marking the extension of the vertical traverse plane onto the cross-section. These profiles are given in Figure 6, as well as pibal wind profiles for Fresno (FRE), which lies a few miles southwest of the Friant VOR beacon and western terminus of the traverses. Profiles of the wind component normal to the Sierras appear in Figure 7, for locations near the traverse line. (The BIH profile, obtained from single theodolite pibal, is of course subject to error due to mountain wave effects.)

A double tropopause structure is evident both days, but not so clearly on the second as the atmosphere has become less stable in the transition zone and more

stable in the troposphere. Upwind of the Sierras wind directions are generally 240° to 260° from crest levels to 60,000 feet. Although the flow at lower levels is stronger the first day some distance upwind and downwind of the Sierras, little difference is noted at FRA or BIH at crest level.

The Scorer parameter was evaluated from the OAK-PGU interpolated temperature/wind profile. Mountain waves are favored where this parameter decreases with height, and surface flow is across the mountains. It is defined at

$$l^2 = \frac{g\beta}{V^2} - \frac{1}{V}\frac{\partial^2 V}{\partial z^2}$$

where $\beta = \frac{1}{\theta}\frac{\partial \theta}{\partial z}$

$V =$ wind component normal to mountains

and the other symbols have their usual meanings.

The Scorer parameter and the two terms on the right are shown versus height in Figure 8, for ML-21 and ML-22. The l^2 curves are basically similar for the two days, with a general decrease up to about 33,000 feet, a slight increase up to about 53,000 feet, and a large increase above.

Plots of U-2 wind directions, wind speeds, and temperatures versus heights for ML-21 and ML-22 appear in Figures 9, 10, and 11, as measured during ascents/descents between traverses, roughly over FRA and TPH. Only one tropopause is evident from the soundings, near 38,000 feet for ML-21 and 42,000 feet for ML-22. The strongest winds on both days occurred near 44,000 feet (which was a traverse level both flights), reaching about 65 knots the first, and 75 knots the second. Directions are nearly all between 220° to 280°,

within about 30° either side of the normal to the Sierra crest. There is a tendency for veering with height. On both days the lowest traverse levels (which determined the base of the soundings) were apparently slightly higher than the lower tropopause shown in Figure 6.

Photographs taken from the U-2 revealed considerable cumulus activity over the Sierras and portions of Nevad.- during ML-21. The cumuli over the Sierras were generally small and ragged in appearance, but a few larger cloud masses were present over the vicinity of the higher peaks. The traverse passed over just such an area on the Sierra crest west of Bishop, where cumulus tops to about 18,000 feet and bases near 13,000 feet were estimated from the U-2 photographic data. A very long and dense band of cirrus and altocumulus was oriented WSW-ENE over EDW, with its northern edge about 40 miles north of EDW. Undulations in this cloud band where it passed over the mountains, and spectacular (as seen from the U-2) lenticular sheets with hard, cobblestone tops indicated wave motions in the southwesterly flow over and to the lee of the mountains north and west of EDW. Some rather flat, but lenticular mid or high clouds were visible far to the north of the traverse route.

The following day, conditions were apparently somewhat drier and more stable since cumulus were very sparse and suppressed. However, during flight ML-22 on that day, the U-2 did fly over extensive sheets of thin high clouds downwind of the Sierra crest, as it proceeded southward from Reno, as far as Mono Lake (40 miles north of the traverse line near Bishop). These clouds were lenticular as seen edge-on from the south, and obviously were associated with

mountain waves.

III. FLIGHT ANALYSES

1. ML-21

1.1 Cross-sections

The analyses which will be presented here for ML-21 cover the multi-level traverse portion of that flight made over the Sierras, and utilize the 1-minute mean data calculated at the University of Dayton. The traverses, eight in all, were carried out within a few miles of each other along a line between FRA and TPH (generally within ±1 mile but as far as ±3.5 miles from the line), and were spaced vertically at five nominally constant levels between about 34,000 feet and 60,000 feet, so that it was possible to perform analyses in a vertical plane across the Sierras. In addition, the last three traverses were repeat runs at the lowest three levels, so that something could be ascertained about time changes in the atmospheric structure.

A well-known technique for diagnosing mountain wave structure from data on a cross-section more or less perpendicular to the mountains is based on assumption of conservation of potential temperature, and steady-state flow non-divergent in the direction normal to the cross-section (parallel to the mountains). In such a situation streamlines of flow in the cross-section and isentropes will coincide. The stratosphere is an excellent place for detection of waves from potential temperature analysis because the very great static stability there assures that vertical displacements of the air are accompanied by relatively strong and unambiguous anomalies in potential temperature. Instead of attempting to draw

the isentropes directly from an x-z plot of the data, it is advantageous to first determine the local departures of the field of isentropes from their altitudes at an upstream reference sounding, in order to isolate the mountain wave perturbations from the large vertical gradients of potential temperature on which they are super-imposed. The analysis of the height departures can then be graphically recombined with the reference values in order to draw the isentropes.

This method was used to obtain an isentrope analysis for the first five ML-21 traverses, illustrated in Figure 12. The upstream sounding was constructed by hand-smoothing plots of U-2 potential temperatures vs height over FRA. The soundings for the TPH end of the traverses were consulted in an effort to eliminate spurious features and fill in missing data. The spacing is nearly constant with x because the reference sounding was assumed to be representative of the entire cross-section. In actuality we would not expect this to be so for the small vertical scale used, because of advection of laminae of various lapse rates and dimensions through the cross-section, and modifications by the mountain waves, but the positions and amplitudes of the waves are nevertheless believed substantially correct. Some movement of the waves took place during the period the cross-section traverses were being flown, as will be discussed later.

The field of isentrope height-departures, from which the above analysis was derived, is shown in Figure 13.

$$\Delta Z_\theta \equiv Z_\theta - Z_r$$

where $\quad Z_\theta =$ height (pressure-altitude) of a particular potential temperature value measured by the U-2

and $Z_r =$ height at which the potential temperature value is found on the reference sounding.

The determination of tilt of the waves was vital to a realistic analysis, since rational interpolation of the analysis between flight levels could not otherwise be carried out. Fortunately, continuous wind information was obtained for nearly the entire flight, so that we could make use of the close relationship between air flow and thermal structure in a mountain wave. If the waves are tilted upstream, the strongest winds should be located downstream of the wave crests, since it is there that streamline (isentrope) packing is greatest; the reverse holds for downstream tilt. An inspection of Figures 17 to 21, in which are graphed the 1-minute means of WS, ΔZ_θ, and other parameters from ML-21, reveals that the faster winds are found preponderantly downstream of maxima in isentrope displacement. Thus, for ML-21, the waves in the region sampled generally tilt upstream. This information was considered in the preparation of Figures 12 and 13.

The wind data was also utilized quantitatively in confirming the analysis prepared from the potential temperature data. It would have been possible to reconstruct the streamline field using only the wind data, as an independent verification of the isentrope analysis. Since graphical methods were employed, it was instead simpler to compare the wind field with the analysis of a quantity derived from the isentrope field as explained below.

Consider a vertical plane x-z which is perpendicular to the mountains. In steady state conditions, the flow in this plane associated with the waves will be nondivergent (neglecting compressibility).
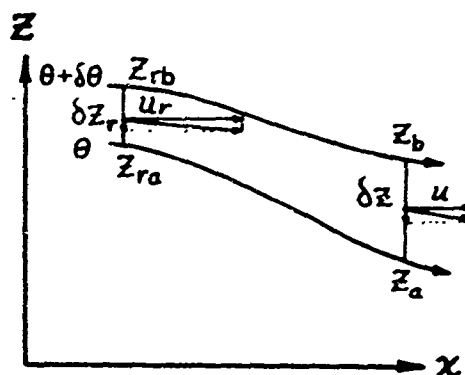
For an isentropic channel of varying height δz (but thin enough so any curvature of the velocity profile is negligible), conservation of mass requires that the component of flow u normal to δz be inversely proportional to the channel height.

That is,
$$u\,\delta z = u_r\,\delta z_r$$

We define
$$\delta z = z_b - z_a$$
$$\delta z_r = z_{rb} - z_{ra}$$

let
$$\Delta z_b = z_b - z_{rb}$$
$$\Delta z_a = z_a - z_{ra}$$

so
$$z_{rb} = z_b - \Delta z_b$$
$$z_{ra} = z_a - \Delta z_a$$

then
$$\delta z_r = (z_b - \Delta z_b) - (z_a - \Delta z_a)$$
$$= (z_b - z_a) - (\Delta z_b - \Delta z_a)$$
$$= \delta z - (\Delta z_b - \Delta z_a)$$

now write
$$\delta(\Delta z_\theta) \equiv \Delta z_b - \Delta z_a$$

then
$$\delta z_r = \delta z - \delta(\Delta z_\theta)$$

and

$$\frac{\delta z_r}{\delta z} = 1 - \frac{\delta(\Delta z_\theta)}{\delta z}$$

but

$$\frac{\delta z_r}{\delta z} = \frac{u}{u_r}$$

$$\therefore \quad \boxed{\frac{u}{u_r} = 1 - \frac{\delta(\Delta z_\theta)}{\delta z}}$$

The wind and isentrope-departure fields can be compared quantitatively if put down in the above form, since the traverse cross-section was nearly normal to the mountains. The left hand side is the ratio of the x-component of the wind to that at the same potential temperature and the same reference location used to evaluate Δz_θ. Because of difficulties in determining u_r as a function of θ at the upwind reference sounding, it was approximated by setting

$$u_r = \overline{u}_L$$

where $\overline{u}_L$ is the mean x-component of the wind for a particular traverse.* An analysis of the speed ratios u/u_r is given in Figure 14. The right hand side of the equation was evaluated graphically (for a δz of 2000 feet). It is shown in Figure 15. In order to facilitate comparison of the two fields, regions where u/u_r and $1 - \frac{\delta(\Delta z_\theta)}{\delta z}$ were less than unity are shown superimposed in Figure 16, using horizontal hatching for the former and vertical for the latter.

---

* The u_L-values are:

level	altitude (feet)	$\overline{u}_L$ (knots)	level	altitude (feet)	$\overline{u}_L$ (knots)
1	33,500	30.6	6	34,000	25.3
2	38,000	36.4	7	38,000	35.2
3	44,000	53.4	8	44,000	55.3
4	52,000	36.6			
5	60,000	20.1			

The two fields are distributed in a similar fashion over most of the region, corroborating the mostly upstream tilt of the waves. If the waves are assumed to extend through several flight levels, there is a very limited number of possibilities for connecting crest or troughs from level to level, half of which are eliminated since nearly all must slope upstream. Of course, the trial $1 - \frac{\delta(\Delta z_\phi)}{\delta z}$ analysis was taken into account when deciding on the connection between different levels in the u/u_r analysis since the two had to be consistent with each other. The solution chosen produced fairly good quantitative agreement between the two fields. Other solutions involve greater slopes away from the vertical, hence would cause an appreciably greater range in the $1 - \frac{\delta(\Delta z_\phi)}{\delta z}$ values and lessen their correlation with u/u_r.

The maximum upwind slope of the waves on the cross-sections is about $z:x = 1:15$, but is closer to $1:5$ on the average. (The vertical to horizontal scale ratio of the charts is $1:15$). As we shall see in the next section, these slopes may differ somewhat from conditions for any given instant, since there was some movement of the waves during the flight. Wavelength is approximately 17 n. miles. The greatest wave amplitudes Δz_ϕ occur directly over the crest of the Sierras, ranging from +2300 feet to -1600 feet. Over the entire cross-section maximum amplitudes occur near 38,000 feet and 52,000 feet.

1.2 Traverse data

Graphs of wind speed, wind direction, ozone, potential temperature, pressure-altitude, and isentrope displacement are displayed in Figures 17 to 21

for each of the eight traverse runs of ML-21. All parameters represent 60-second averages, except ozone, which is plotted at its rate of sampling, about three per minute. Turbulent periods are marked by shading. Since the three lowest levels were repeated, a double set of curves appear on these graphs, with the later runs shown as dashed lines. Arrows on the Z_p trace indicate direction of flight.

Some interesting interrelationships can be pointed out between the various parameters. If the perturbations in θ are nearly stationary, they are indicative of mountain waves, with rising motions upwind of the crests and sinking downward. Considering that the pilot or autopilot will be attempting to keep the aircraft near the nominal flight level, there are definite indications that the aircraft is responding to these alternating up and down winds. Aircraft altitude variations due to the waves should be in-phase with ΔZ_θ for flight with the flow (left to right in the diagram), 180° out-of-phase against the flow. The greater oscillations in altitude tend to occur during upwind flight since a longer time is spent flying upwind through the waves. As has been earlier mentioned, wind speeds were usually stronger downwind of crests, indicating that the waves slope upward upstream. Ozone becomes more variable with distance as its concentration increases upwards. It is well correlated with potential temperature but not aircraft altitude along the upper flight levels, which constitutes additional evidence that the air has been displaced upwards and downwards in the waves. It is difficult to relate variations in wind direction to the waves. When the direction of the flow entering the wave region is at an appreciable angle to the normal to the waves (presumed 255°-075°) some of the

acceleration experienced by the air as it passes through the waves should be manifest as a turning towards the downstream normal direction with increasing speed, away for decreasing. Put another way, the velocity component parallel to the waves should remain constant if the waves are laterally uniform, and the normal component will oscillate. A polar scatter diagram of the vector wind was plotted (not shown) for the traverse winds, but there was only fair tendency for alignment of the end points along a line perpendicular to the waves.

Movement and modification of the mountain wave structure can be seen in the ΔZ_θ -curves at the repeated three lowest levels. During the 2-3 hour period between the first and second set of traverses the first major crest has shifted to (or reformed at) up to 7-8 miles upstream of its earlier position. It is hard to say what happened to most of the downstream waves because of uncertainty as to identity. If this displacement occurred at all levels, the waves at 60,000 feet shown in the cross-sections would have been about 5 miles further downwind relative to the positions at 34,000 feet, so that the waves would in general slope more towards the vertical than analyzed. Slopes of those portions of waves closest to vertical would be affected most; 1:15 would go to 1:14, 1:5 to 1:4, 1:1 to vertical, and those originally analyzed between 1:1 and vertical would slope downwind. The lines of equal isentrope displacement, ΔZ_θ would be rotated clockwise in the diagrams. Since the field of $1 - \dfrac{\delta(\Delta Z_\theta)}{\delta z}$ would thus be altered, the discrepancies between it and u/u_r might be alleviated if it were possible to correct the analyses to a standard time. This was not attempted here because of the uncertainty in identifying

corresponding features between the two sets of traverses, and the lack of repeat runs at the higher levels.

1.3 Turbulence

The episodes of turbulence indicated by the accelerometer records are shown as short zigzag symbols on the cross-sections, and by shading on the traverse data graphs. Turbulence was observed at the 44,000-foot (maximum vertical acceleration 0.21g), 52,000-foot (0.35g), and 60,000-foot levels (0.65g and 0.35g). The pilot reported that turbulence at the highest level was the most impressive he had ever experienced. Some turbulence described as "light" was observed by the pilot over the western slope of the Sierras, but was not included with that detected by the accelerometer. It will be noted that the three strongest turbulent occurrences all took place just downstream of wave troughs. This fact will be examined in more detail later.

2. ML-22

2.1 Cross-section

A cross-section of Δz_{θ} for ML-22 is shown in Figure 22. These values are based on an upstream reference sounding constructed from U-2 ascent/descent data in the same manner as for ML-21, but in this case were obtained for 5-second intervals, along the traverses, and then smoothed by hand. Detection of the phase of wind speed fluctuations relative to Δz_{θ} in order to verify the direction of wave slope proved rather uncertain and ambiguous in this case.

An analysis of u/u_r was not attempted. Nevertheless the waves were analyzed

tilting upstream as on the previous day. The slopes were roughly the same as

before. The uppermost traverse (67,000 feet) was not included because we could

not establish the analysis in that region with any confidence. This is probably

in part due to the fact that that level was flown last, much later than the one

below it, as can be seen from Figure 2. The wave amplitudes are considerably

less than the previous day. The greatest amplitudes are found in the vicinity of

38,000 feet, and 52,000 feet, and over and downwind of the White Mountains.

Maximum displacements are +1200 and -1400 feet. The predominant wave-

length remains at about 17 n. miles. On the whole the ML-22 cross-section

seems less organized than the similar one for ML-21; this appearance stems partly

from imperfect filtering of the shorter perturbations in the hand-smoothing process

employed. The diminished convective activity on the 14th could also be a factor,

since it suggests less disturbance of the tropospheric cross-mountain flow than on

the previous day.

2.2 Horizontal temperature analysis

During flight ML-22 several legs were flown near 60,500 feet, suggesting

an attempt to reconstruct the wave pattern at that level. Since only in the vicinity

of the traverses were soundings available from which the details of the vertical

potential temperature distribution could be determined, we did not think it worth-

while to attempt to compute ΔZ_θ. However, in a gross sense, the temperature

lapse rate in the stratosphere was isothermal, which meant that variations in

temperature along the 60,500-foot flight track would hopefully tend to reflect
actual horizontal temperature changes, and not so much changes in altitude of
the U-2 as it deviated somewhat above and below the nominal flight altitude.
(Actually, temperature and $\Delta z_\bullet$ compared quite well during the traverse at
60,500 feet; see Figure 29.)

An analysis of the horizontal temperature distribution appears in
Figure 23. The data was smoothed subjectively to remove small-scale fluctuations.
Unfortunately, the solution has to be regarded as somewhat speculative, at least
between the traverse line and Reno, since the temperature data alone would allow
giving the features other orientations. The version given, however, is consistent
with the existence of mountain waves, for which there was considerable evidence.
The axes of the colder areas are presumed to mark wave crests, where the air has
been displaced upwards and hence cooled adiabatically; the warm axes likewise
mark troughs.

The wind from the surface through flight level was southwesterly, so the
features shown are roughly perpendicular to the flow, and parallel to the Sierras.
The wavelength indicated is about 17 n. miles near Bishop, to 40 n. miles near Reno.

2.3 Turbulence

All of the turbulence noted for ML-22 occurred at the 60,500-foot level,
at the locations shown by the large dots in Figure 23, and one of the locations by
the zigzag symbol in Figure 22. Maximum accelerations between 0.30g to 0.64g
were measured, comparable with the previous day, but there was only one

accelerometer report of turbulence during the traverses, at about 2210 GCT over

the White Mountains. A pilot report of "turbulence over valley" at 2208 GCT

was made, however there is some doubt a separate incident was involved because

the pilot's clock may have been as much as two minutes behind that used in the

instrumentation package. Again, the correspondence between strong turbulence

occurrences and wave troughs is pointed out.

IV. WAVE STRUCTURE AND TURBULENCE

1. Observations

An association between the turbulence and wave troughs has been indicated.

In order to look further into this, pertinent portions of ML-21 and ML-22 were examined,

using unsmoothed 5-second data.

Figures 24 to 26 are graphs for ML-21 of various flight parameters versus

distance along the FRA-TPH coordinate, similar to Figures 17 to 21 shown earlier

except for the smaller time scale depicted. In the 52,000-foot episode, Figure 24,

the turbulence was confined to mid-trough and a region slightly downwind (according

to Δz_e), beginning just after a rapid decrease in wind speed and ceasing approximately

in the region where speeds began to rise again. Remembering that at this level the

U-2 was flying upwind, from right to left on the graph, note the rapid increase in

altitude as the aircraft entered the area upwind of the wave crest. It is tempting

to relate the subsequent drop to the turbulent zone, and the abrupt change in $\Delta \dot{z}_e$

at 2240 GCT, but it may well have merely reflected the pilot's attempt to bring

the aircraft back to the nominal flight altitude. The possibility that the pressure-altitude was merely responding to strong horizontal variations in pressure is not borne out by the behavior of the wind speeds.

The next encounter was the most severe ($\leq 0.65g$), Figure 25. It took place at 60,000 feet where the U-2 was flying downwind, left to right on the graph. The turbulence began just before the lowest point in the trough, and died out in the vicinity of the next downstream wave crest. The rise in U-2 altitude during its passage from trough to crest suggests a strong upward flow there, implied by the increase in isentrope altitude (from ΔZ_θ). The spectacular dips in amplitude of the trough to departures below -3000 feet may be partly due to an inaccurate θ reference profile; the behavior of the "undisturbed" upstream potential temperature sounding had to be extrapolated for $\theta > 456^\circ K$ since the U-2 did not go high enough to measure it.

Another region of strong turbulence was found 50 miles farther downwind, at 60,000 ft., Figure 26. It began at a speed minimum, in the center of the wave trough, and also died out near the following wave crest.

Similar graphs have been prepared for ML-22, except that a time scale is employed since distances along the flight legs were not obtained from the computer. However, for ease in comparison, the charts have been drawn with a horizontal scale roughly equivalent to that of ML-21 charts. The first two occurrences took place when the U-2 was flying south from Reno at a small angle to the waves, heading slightly upstream. The wave topography will have to be inferred from the temperature

curve, since, as mentioned earlier, no U-2 sounding data was obtained in this region. Figure 27 illustrates data during the turbulence just south of Reno. The coincidence of warmer temperatures (temperature is plotted increasing downwards in order to be similar to ΔZ_θ) and turbulence implies a trough turbulence relationship, as before. Note that time is plotted from right to left in order to have the upstream direction to the left, as in all the other illustrations. This puts the upstream edge of the turbulent zone squarely on the wave trough, according to the temperature curve. The wind speed minimum and U-2 altitude maximum at the trough conform to their expected behavior in a mountain wave.

Near Mono Lake the heaviest turbulence of the flight was experienced, Figure 28. Wind speed may not be reliable; part of the time the Doppler radar was not tracking properly. However, temperature, turbulence, and U-2 altitude behave in a consistent manner, as before. The separation of the turbulence, and trough topography (temperature) into two parts is probably due to lateral variations in the wave seen by the aircraft because of the small angle of crossing.

Finally, in Figure 29 we show the portion of the flight at 60,000 feet over the White Mountains. Here it was possible to compute ΔZ_θ, and the very close resemblance between it and the temperature supports our previous topographical interpretation of the latter. The turbulence, here also, is confined to the region between a trough and next downstream crest.

2. Discussion

The region between wave trough and downstream crest has been shown to be the site of all but one of the strong accelerometer-identified espisodes of turbulence during ML-21 and ML-22. Some possible reasons for this near-exclusive behavior will be discussed below.

Static-stability in upwind-tilted waves is least on the downstream side of the troughs, where the isentropes have been tilted and stretched vertically in the decelerating flow, and at altitudes where the wave amplitude is at a local maximum. It is possible for the isentropes to become increasingly inclined so that vertical mixing and turbulence take place. This instability may be carried to the point of actual undercutting by the flow entering a trough from the speed maximum or its upwind side, so that a disturbance resembling a hydraulic jump develops.

An important factor which should be investigated is the distribution of Richardson number. The mountain wave structure can be shown to influence Ri in a very interesting manner, because of the relationship between shear and static stability in the waves. Consider an idealized two-dimensional mountain wave situation in vertical cross-section:

The horizontal component of flow u in the x-direction within an isentropic channel of infinitesimal height can be written (neglecting compressibility)

$$u = b u_r \tag{1}$$

where
$$b \equiv \frac{(\partial z / \partial \theta)_r}{\partial z / \partial \theta} = \frac{\partial z_r}{\partial z} \tag{2}$$

The subscript r here and following denotes parameters measured at some reference location in the undisturbed flow upstream of the mountains, at the potential temperature of the point of the cross-section under consideration. The parameter b expresses the amount of vertical compression or expansion of the isentropic channels relative to their vertical distribution at the upstream reference location; this is a function of x, and z or θ, and will vary depending on wave slope and amplitude.

We would like to express the Richardson number in terms of the above conditions.

We have

$$Ri = \frac{\frac{g}{\theta}\frac{\partial \theta}{\partial z}}{\left(\frac{\partial u}{\partial z}\right)^2} \qquad (3)$$

where

$$u = u(x, \theta) \qquad (4)$$

$$\theta = \theta(x, z) \qquad (5)$$

Differentiating (1) wrt θ at some x,

we have

$$\frac{\partial u}{\partial \theta} = b\left(\frac{\partial u}{\partial \theta}\right)_r + u_r\frac{\partial b}{\partial \theta} \qquad (6)$$

but

$$\frac{\partial u}{\partial \theta} = \frac{\partial u}{\partial z}\frac{\partial z}{\partial \theta} \,, \quad \left(\frac{\partial \theta}{\partial z}\right)_r = \left(\frac{\partial u}{\partial z}\right)_r\left(\frac{\partial z}{\partial \theta}\right)_r \,, \quad \frac{\partial b}{\partial \theta} = \frac{\partial b}{\partial z}\frac{\partial z}{\partial \theta} \qquad (7)$$

substituting,

$$\frac{\partial u}{\partial z}\frac{\partial z}{\partial \theta} = b\left(\frac{\partial u}{\partial z}\right)_r\left(\frac{\partial z}{\partial \theta}\right)_r + u_r\frac{\partial b}{\partial z}\frac{\partial z}{\partial \theta} \qquad (8)$$

$$\frac{\partial u}{\partial z} = b\left(\frac{\partial u}{\partial z}\right)_r\frac{(\partial z/\partial \theta)_r}{\partial z/\partial \theta} + u_r\frac{\partial b}{\partial z} \qquad (9)$$

but $\qquad b = \dfrac{(\partial z/\partial\theta)_r}{\partial z/\partial\theta}$ $\qquad\qquad$ (10)

$\therefore\ \dfrac{\partial u}{\partial z} = b^2\left(\dfrac{\partial u}{\partial z}\right)_r + u_r\dfrac{\partial b}{\partial z}$ $\qquad\qquad$ (11)

From (10) $\quad \dfrac{\partial\theta}{\partial z} = b\left(\dfrac{\partial\theta}{\partial z}\right)_r$ $\qquad\qquad$ (12)

Substitute (11) and (12) in (3):

$$Ri = \frac{\frac{g}{\theta}\, b\left(\frac{\partial\theta}{\partial z}\right)_r}{\left[b^2\left(\frac{\partial u}{\partial z}\right)_r + u_r\frac{\partial b}{\partial z}\right]^2} \qquad\qquad (13)$$

This expression may be used to draw some inferences about probable turbulence generation sites in the waves, although it is probably not valid for strongly inclined flow or shear.

There are several means by which mesoscale changes in vertical gradients of potential temperature and velocity, leading to decreasing Richardson numbers and turbulence, may occur. One way is through differential advection. Another is through vertical shrinking of an air column due to horizontal divergence, since the increase in static stability is overcompensated by the effect of shear, which appears squared in the demonimator for Ri. With the wealth of small-scale variations in shear and stability present in the atmosphere, it can be seen that even large-scale divergence fields, if persisting for some time, could serve to bring the Ri of some of these regions to the critical point, perhaps at many locations over a wide area.

When the divergence field producing the vertical shrinking is stationary, the effect is the same, but much more intense. Consider diagrams a) and b).

In this situation a simple wave, damped with height, is present directly over an obstacle. Suppose, for simplicity, that the shrinking is constant with height, and is sufficient to compress the interval between isentropes θ and $\theta + \delta\theta$ to one-half their former spacing at r. Then the static stability will have doubled. But wind speeds will also have doubled, whereas since the spacing is halved, the shear will have quadrupled. The Richardson number which was characteristic of the upwind profile will have changed by a factor of 2 (twice as stable in numerator) divided by 4^2

(shear squared in denominator), or a factor of $1/8$. This result can be obtained

from the mountain-wave form of the Richardson number:

$$Ri = \frac{b \frac{g}{\theta} \left(\frac{\partial \theta}{\partial z}\right)_r}{\left[b^2 \left(\frac{\partial u}{\partial z}\right)_r + u_r \frac{\partial b}{\partial z}\right]^2}$$

by setting $\frac{\partial b}{\partial z} = 0$, since we have assumed the shrinking constant with height,

and b is a measure of that shrinkage.
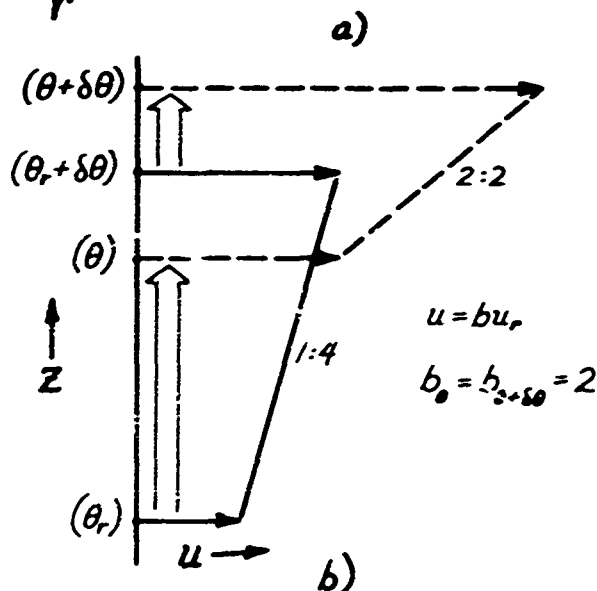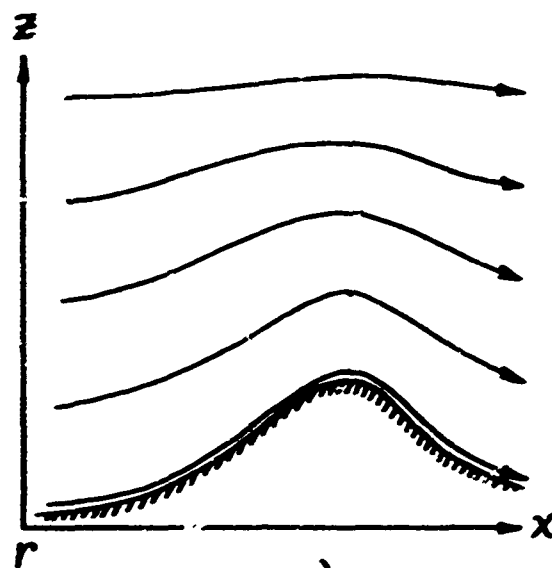
Then, $$Ri = \frac{b \frac{g}{\theta}\left(\frac{\partial \theta}{\partial z}\right)_r}{\left[b^2\left(\frac{\partial u}{\partial z}\right)_r\right]^2}$$

Therefore, for a non-sloping wave whose amplitude changes linearly with height,

$$Ri = \frac{\frac{g}{\theta}\left(\frac{\partial \theta}{\partial z}\right)_r}{b^3\left(\frac{\partial u}{\partial z}\right)_r^2}$$

but $$\theta = \theta_i.$$

$$\therefore Ri = b^{-3}(Ri)_r$$

where $(Ri)_r$ is the Richardson number at the same θ-level on the upwind sounding.

In the general case, the waves tilt and their amplitudes vary with height. Considering the effect of the tilt, it serves to make b periodic with height. For given wave amplitudes, as they slope more toward the horizontal the greater the amplitude of b will vary. Zones of minimum Ri will tend to prevail either side of sloping speed maxima upwind of upwind-sloping wave troughs, since it is there that $\frac{\partial b}{\partial z}$ will attain its greatest magnitude. The effect of shear in the upstream profile will be to minimize Ri just below the sloping wave speed maxima for positive shear, and above for negative shear. Suppose that conditions are such that critical values of Ri are being produced by the effect of the wave structure upon the incoming air in this manner. If the static stability downstream is only marginally stable, small-scale disturbances forming in these sloping zones of minimum Ri and being advected into the trough could act to set off turbulence there. It may be significant that the smallest Ri-values are on the trough side
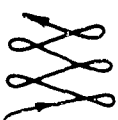
of the speed maxima, above the level of maximum wind, since all strong turbulence in ML-21 and ML-22 was encountered in the upper levels where generally negative shear prevailed. Below the level of maximum wind Ri may have become critical only below the wave speed-maxima; the disturbances would then have had to survive passage through a region where Ri was relatively large before reaching the trough.

V. CONCLUDING REMARKS

Data from flights ML-21 and ML-22 have been used to construct mesoscale analyses of mountain waves in the stratosphere, and to establish observational evidence for an intriguing connection between turbulence distribution and wave structure. With the hindsight gained from attempting to correctly interpret and utilize the data, some comments pertinent to flights of this type will be offered.

1. Accurate recovery of the aircraft positions is necessary, because of the link between terrain and mountain-wave locations and need for correct vertical alignment of multi-level traverses. Positions should be determined from the tracker camera photos (assuming, hopefully, clear skies below) and used instead of the VOR over-flights, for reference positions at suitable intervals throughout the flight.

2. For analysis of gross wave structure, the traverse data should be smoothed by a running mean of between 30 to 45 seconds duration (appropriate for normal U-2 ground speeds).

3. Emphasis should be placed on obtaining at least one complete, uninterrupted, upwind profile of temperature, wind speed, and direction. (If possible, one complete upwind sounding at the start of and another at the end of the traverses.) The aircraft should descend as low as time and clearance will permit. The upper terminus of the sounding (s) must extend at least several hundred feet higher than the elevation of the highest traverse level, perferably a few thousand feet.

4. Anytime flight levels are changed, extend the ascent/descent to overlap the beginning and ending levels by at least several hundred feet, in order to be able to determine vertical gradients to be used for the flight levels.

5. Most of the losses of wind data occurred during helical ascent/ descent apparently because of too steep a bank or inclination. To obtain an uninterrupted wind sounding, it is suggested that the aircraft change elevation in a series of "vertical switchbacks", attempting to stay within the vertical plane of the traverse route. The switchback maneuver for a descent would involve leveling out fully (so at least one tracker camera photo readily useable for positioning could be obtained), then a climb of a few hundred feet (to insure overlap between the switchbacks), a sharp turn to reverse direction, and resume descent.

6. With the exception of the region where significant mountain waves are being encountered, a vertical porpoising maneuver is preferable to quasi-horizontal flight because of the valuable information gained as to vertical distribution of atmospheric laminae and horizontal variation of their strength and height. The more rapid and steep the porpoising, the smaller the horizontal scale of features discernable, however, unless some wind data can be sacrificed the ascent/descent rate must be kept within certain limits.

7. Repeat runs should be made at all levels if possible. Multiple, consecutive repeat runs at at least one level should be made in order to be able to separate moving features from the more nearly stationary mountain waves.

8. Flight to and from the traverse area should not be made direct but, if time permits, planned in a zigzag manner (with at least occasional porpoises) with legs over the mountains, so that the horizontal configuration of the waves can be determined. The return flight should be at the same level as the departing flight.

9. Lateral variations in wave structure should be checked in some smaller, selected region, by a series of at least three adjacent (2-5 miles separation) and consecutive passes (20-30 miles in length), or a crisscross pattern gradually progressing in a direction parallel to the mountains. The latter pattern has the advantage that time changes may be detected at the crossover points.

Realizing that all of the above are probably more than any one aircraft is capable of handling within a reasonable time period, and that some may not be practicable at all, it is nevertheless believed that adoption of the suggestions relating to determination of vertical structure would prove especially beneficial.
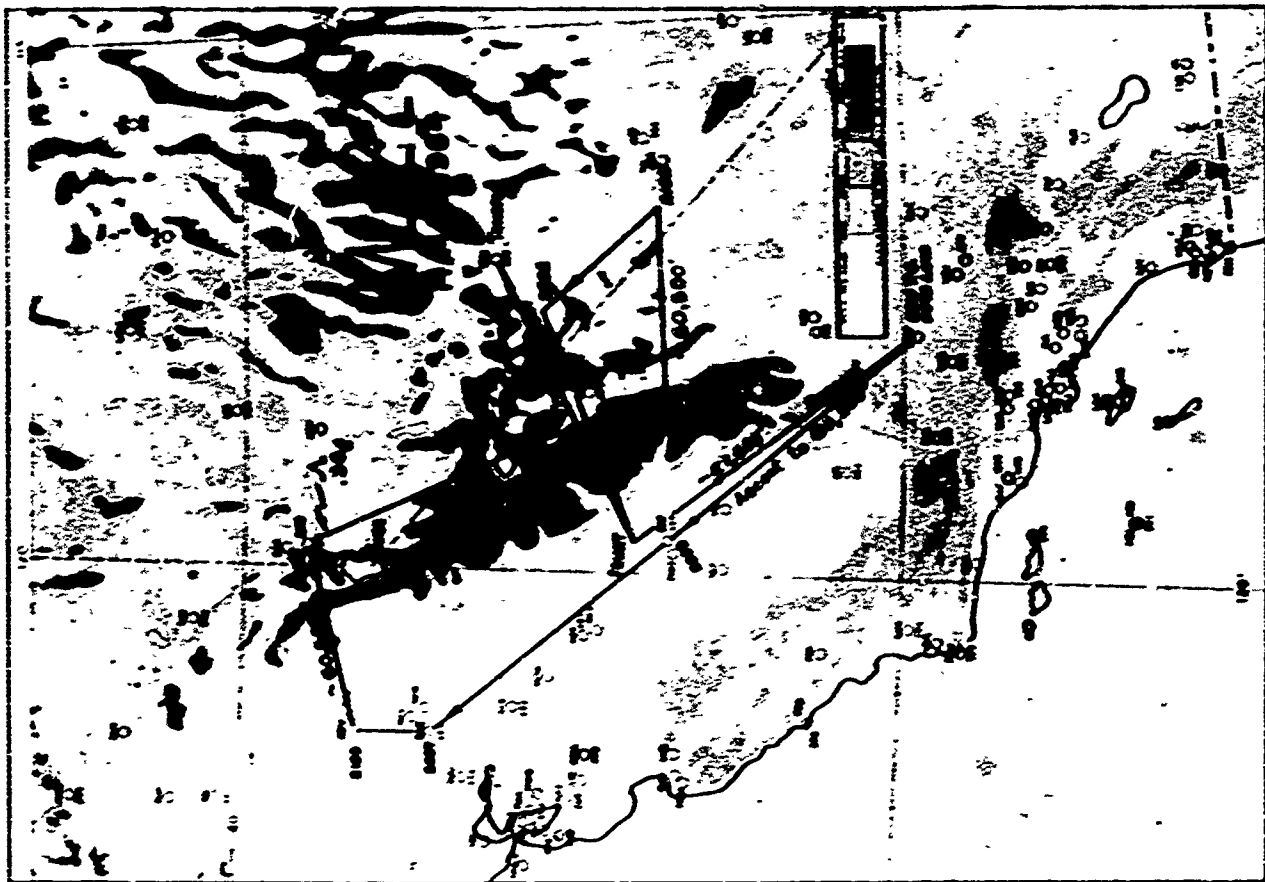
FIGURE 2a.   Traverses, ML-21.
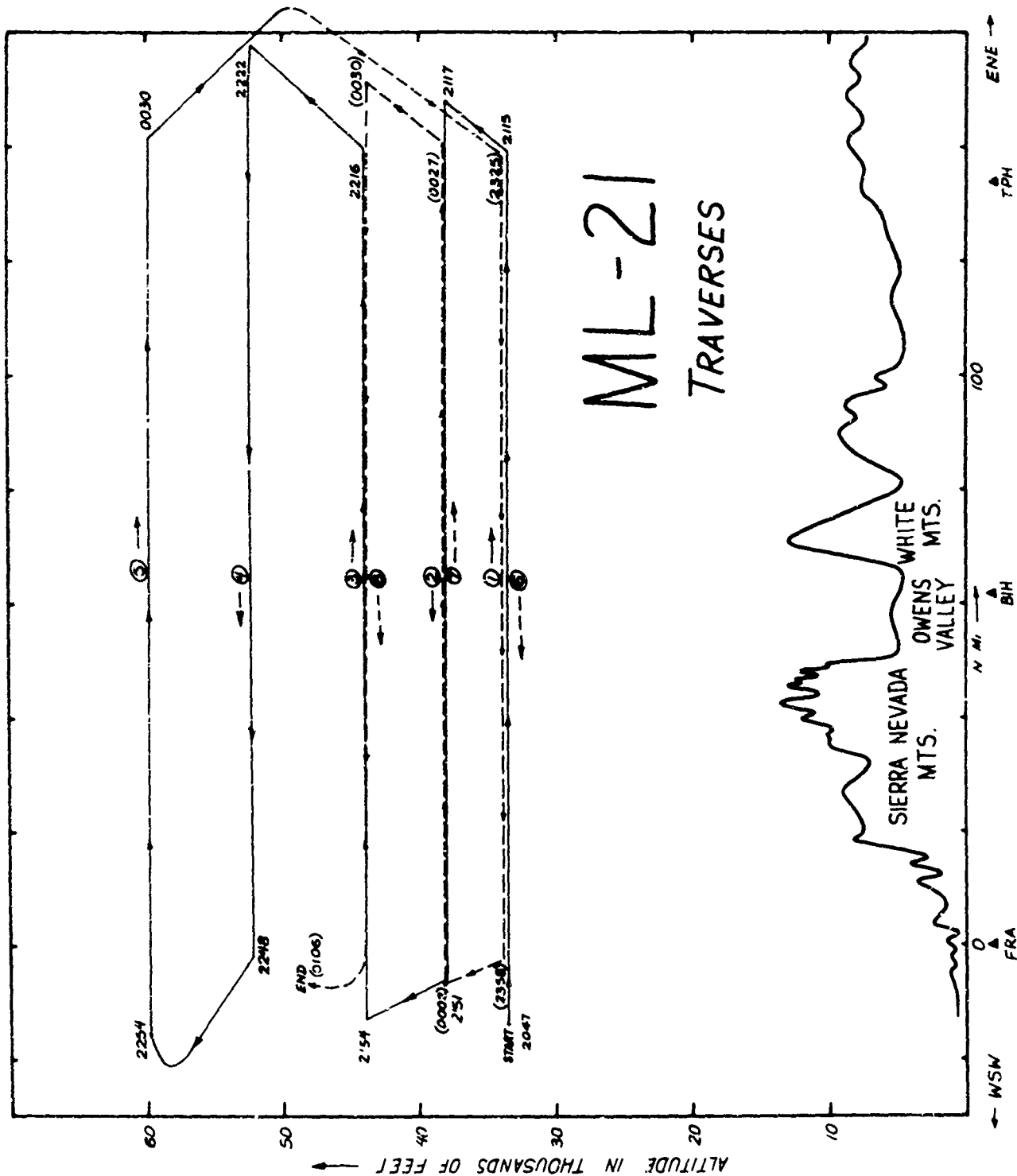
ML-21
TRAVERSES

FIGURE 2b.   Traverses, ML-22.

ML-22

TRAVERSES

START 2202

END 1000

2249

2219

2222

2242

2309

2311

2312

2314

234

SIERRA NEVADA MTS.

OWENS VALLEY

WHITE MTS

← WSW

ENE →

N. M. →

FRA

BIH

TPH

100

ALTITUDE IN THOUSANDS OF FEET

60

50

40

30

20

10
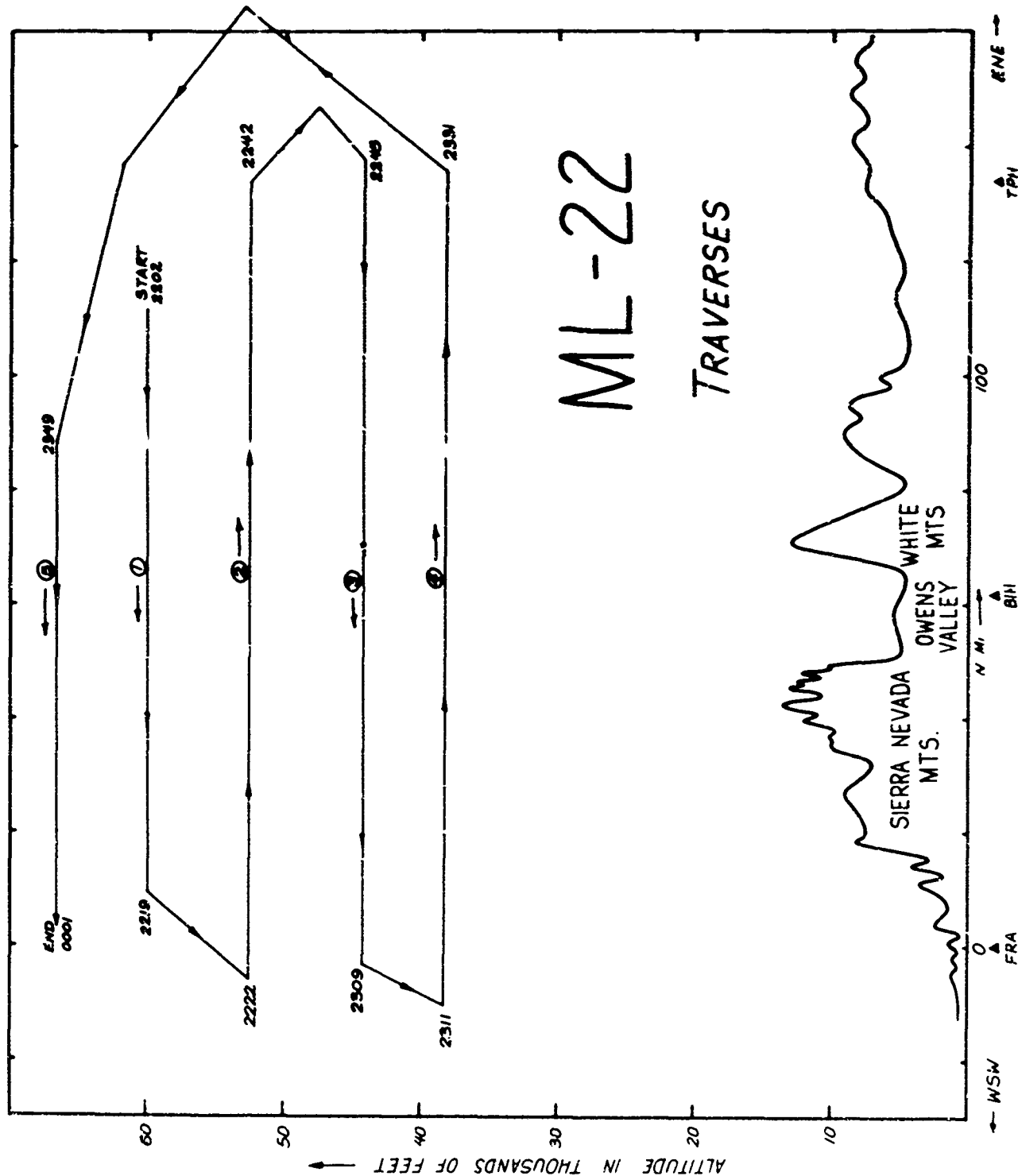
FIGURE 3.   Winds aloft during ML-21 and ML-22.

00 GCT 14 and 15 May, 1964.

Dashed lines are isotachs in knots.

Solid lines are streamlines.

ML-21
00Z 14 MAY 64
70 mb
~60,000 FT.

ML-22
00Z 15 MAY 64
70 mb
~60,000 FT.

300 mb
~30,000 FT.

300 mb
~30,000 FT.

700 mb
~10,000 FT.

700 mb
~10,000 FT.
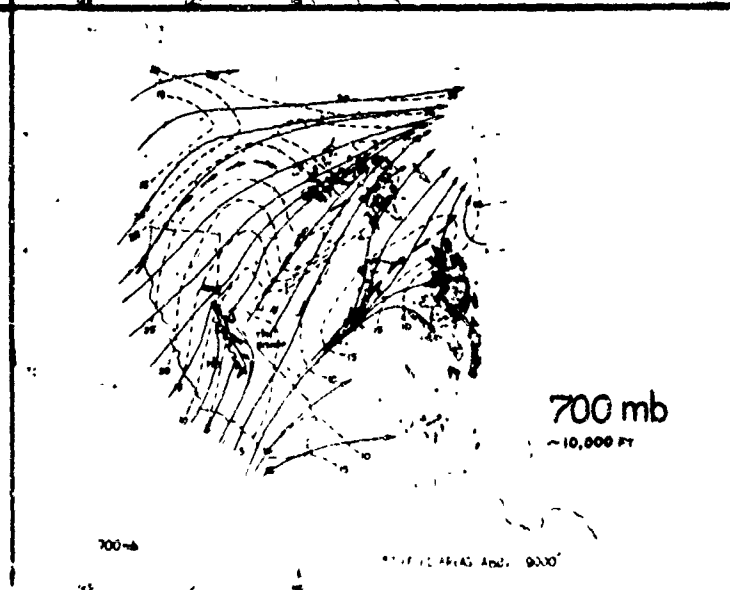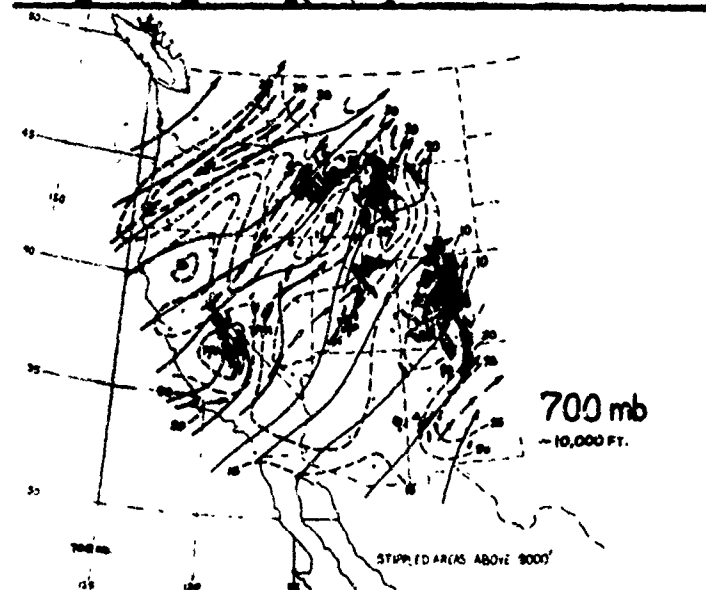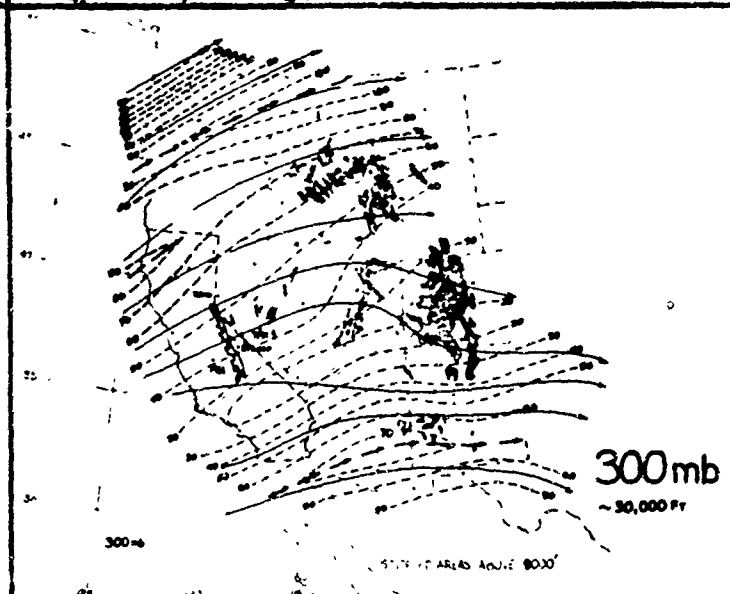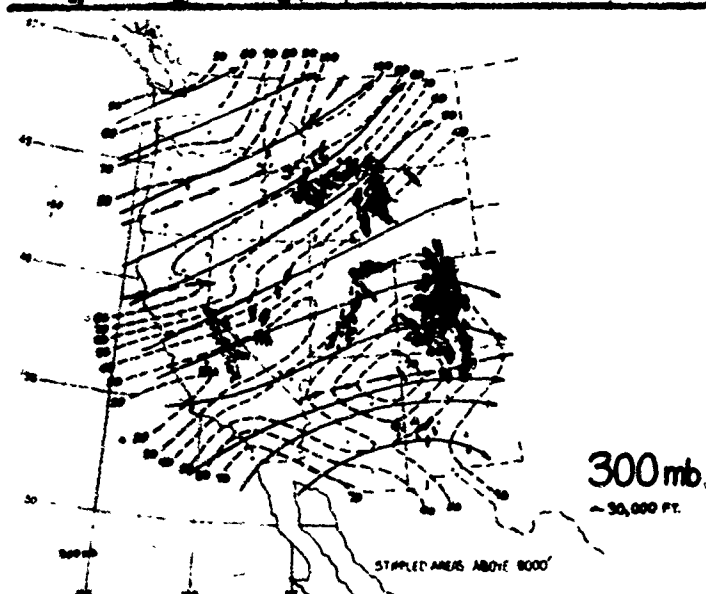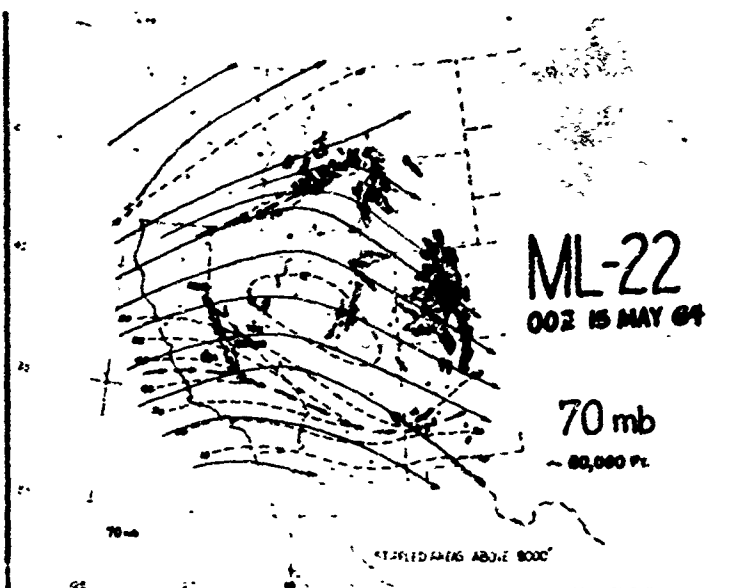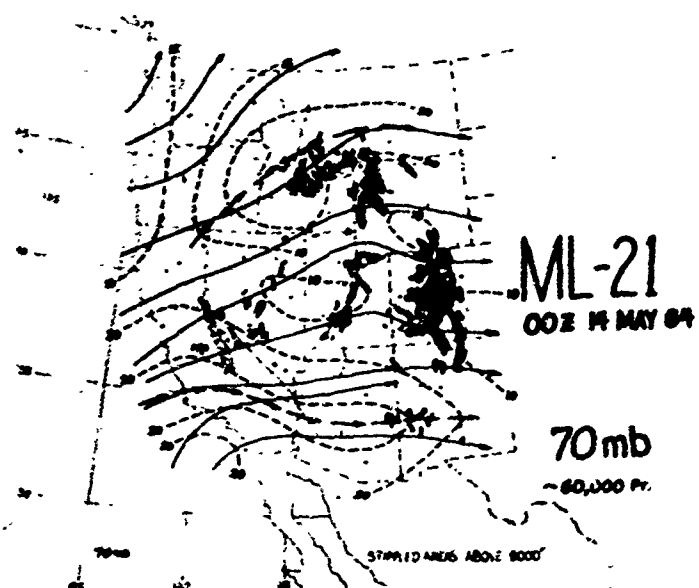
FIGURE 4.   Vertical cross-section along Pacific Coast

during ML-21.

00 GCT 14 May, 1964.

Heavy dashed lines are tropopause or stable layer

boundaries.

Light dashed lines are isotachs in knots.

Heavy solid lines are isentropes in deg K.

Light solid lines are isogons.

ISENTROPE (°K) ―――― 270 ISOGON ―――― ⊗ ISOTACH (knots) ML-21 00 z 14 MAY 1964
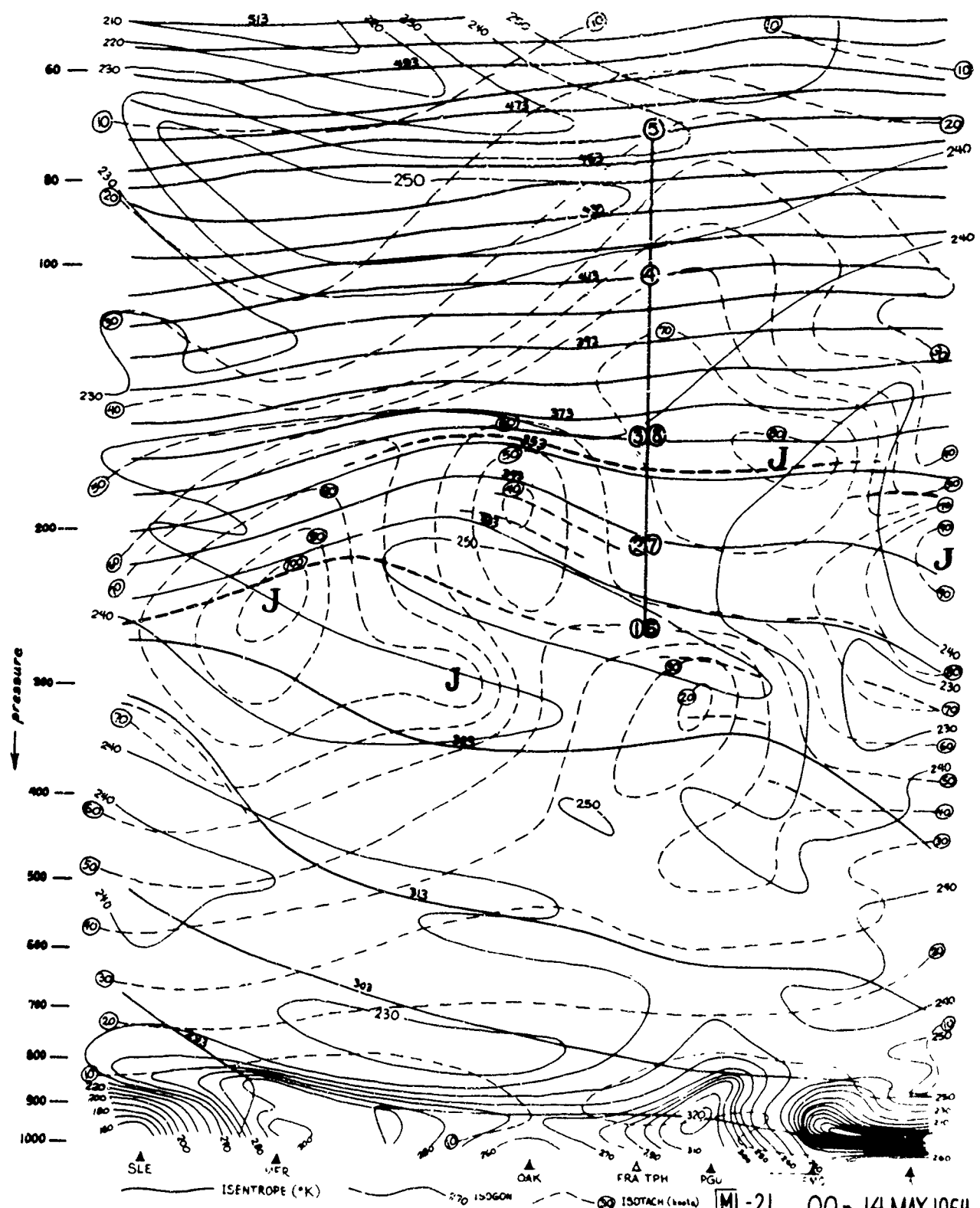
FIGURE 5.   Vertical cross-sections along Pacific Coast

during ML-22.

00 GCT 15 May, 1964.

Lines same as for Figure 4.

ISENTROPE (°C)   ISOTACH knots.   ML-22   00z 15 MAY 1964
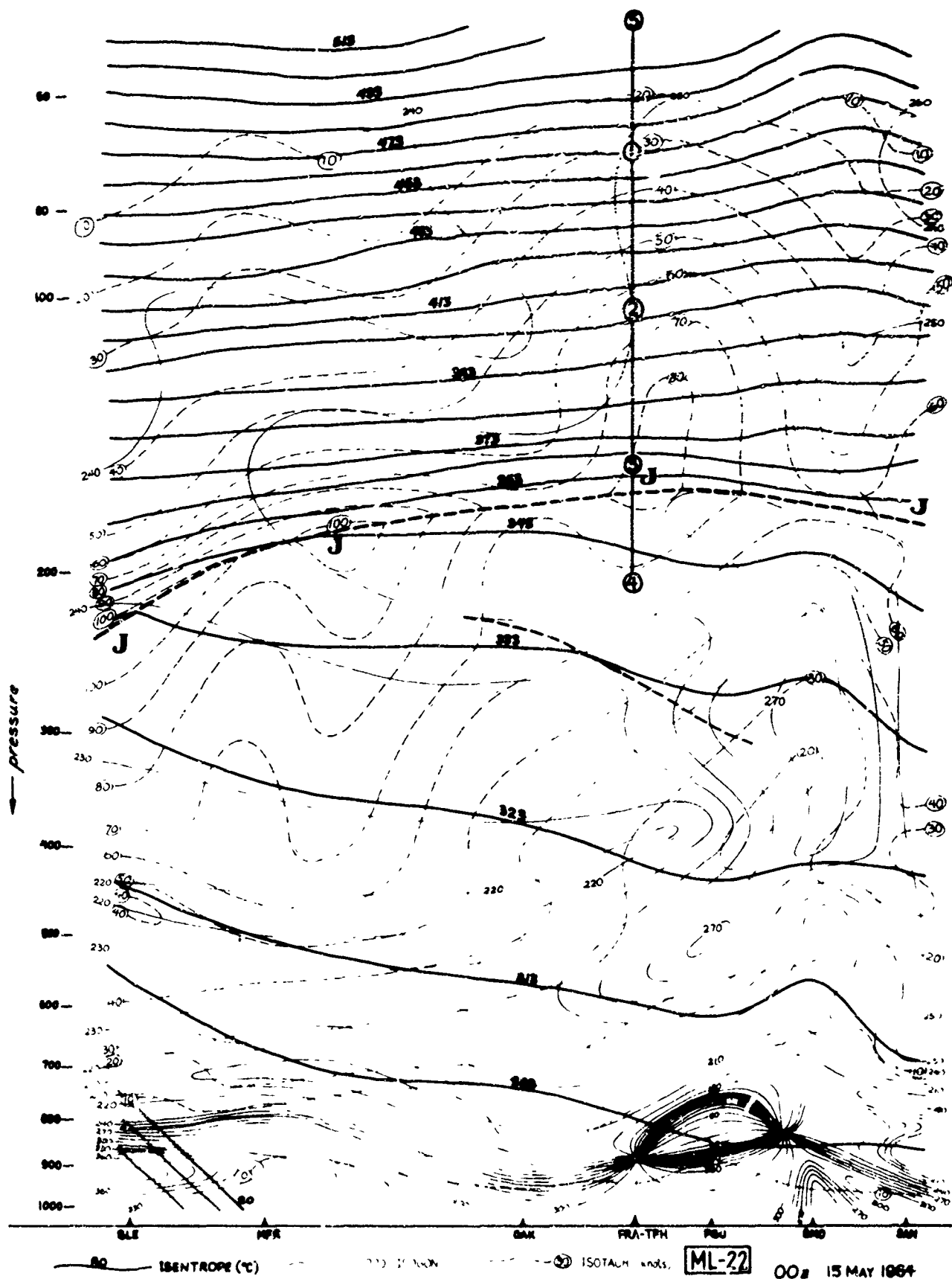
FIGURE 6. Left diagram: Interpolated temperature profiles

upstream of traverse route, for ML-21 and ML-22.

Right diagram: Interpolated wind soundings upstream

of traverse route, and from Fresno pibals, for ML-21

and ML-22.

Light lines are for 00 GCT 14 May, 1964.

Heavy lines are for 00 GCT 15 May, 1964.

Solid lines are interpolated profiles.

Dash-dot lines are for Fresno.

ML-21
ML-22

SPEED

DIRECTION

Wind Speed (Knots)
Wind Direction

USAF SKEW T, log p DIAGRAM
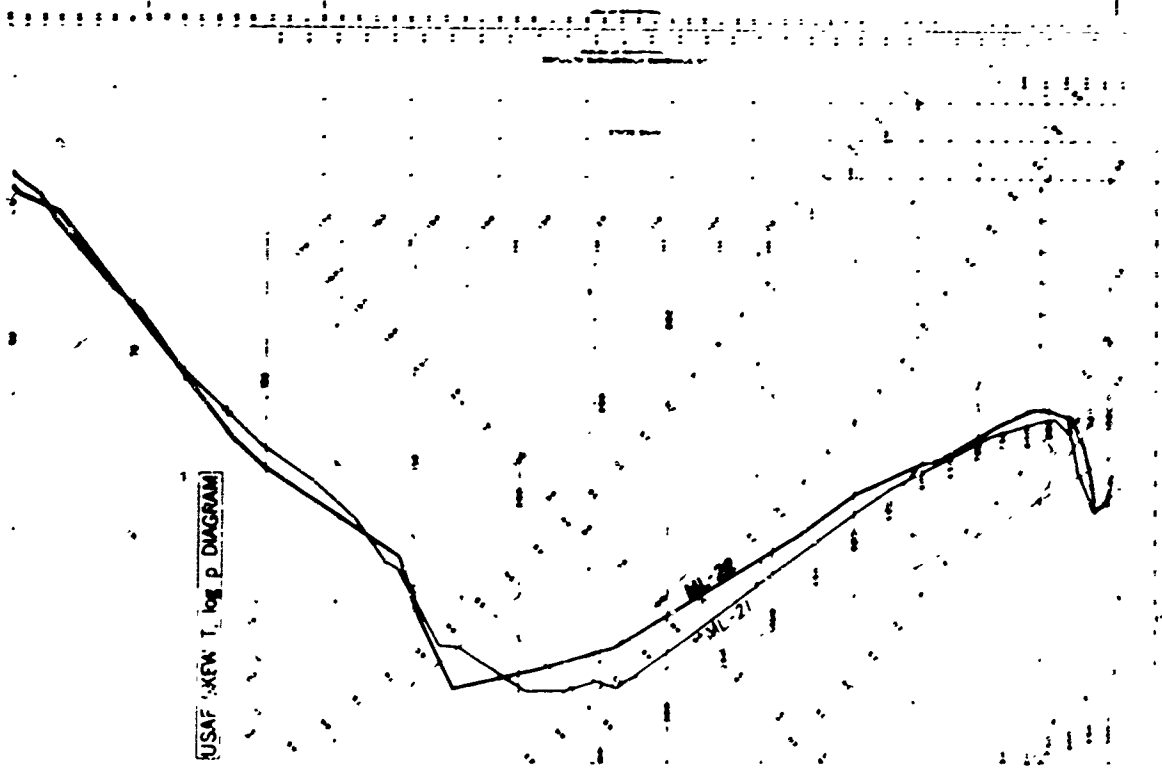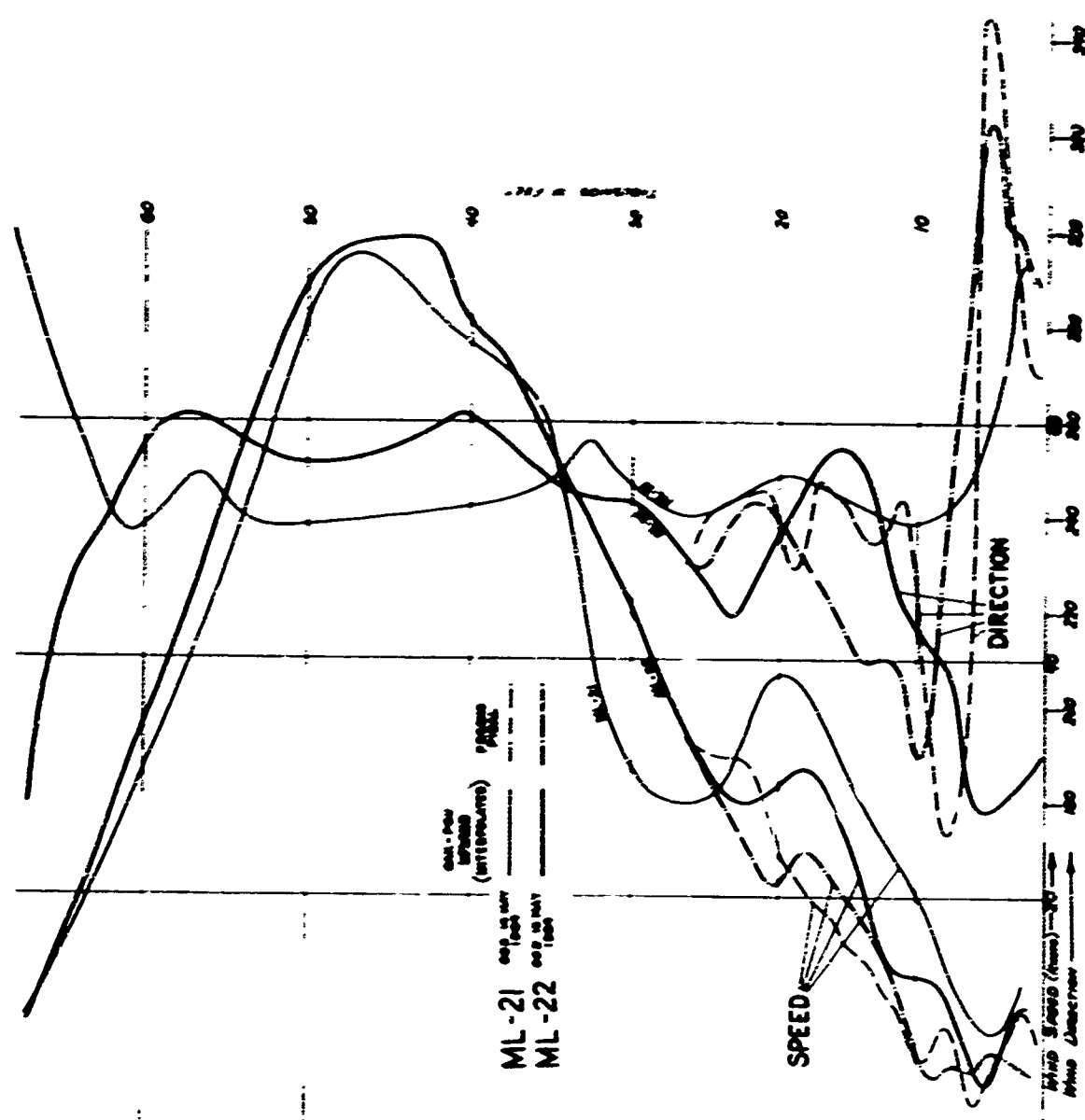
FIGURE 7.   Profiles of wind component perpendicular to Sierras,

for locations near axis of traverse route.

Light lines, 00 GCT 14 May, 1964.

Heavy lines, 00 GCT 15 May, 1964.

WIND COMPONENT
FROM 255°
(~⊥ SIERRAS)

00Z 14 May —— ML-21
00Z 15 May —— ML-22

50 KNOTS

10 KNOTS

OAK/PGU   FAT   BIH   (TPH)   ELY
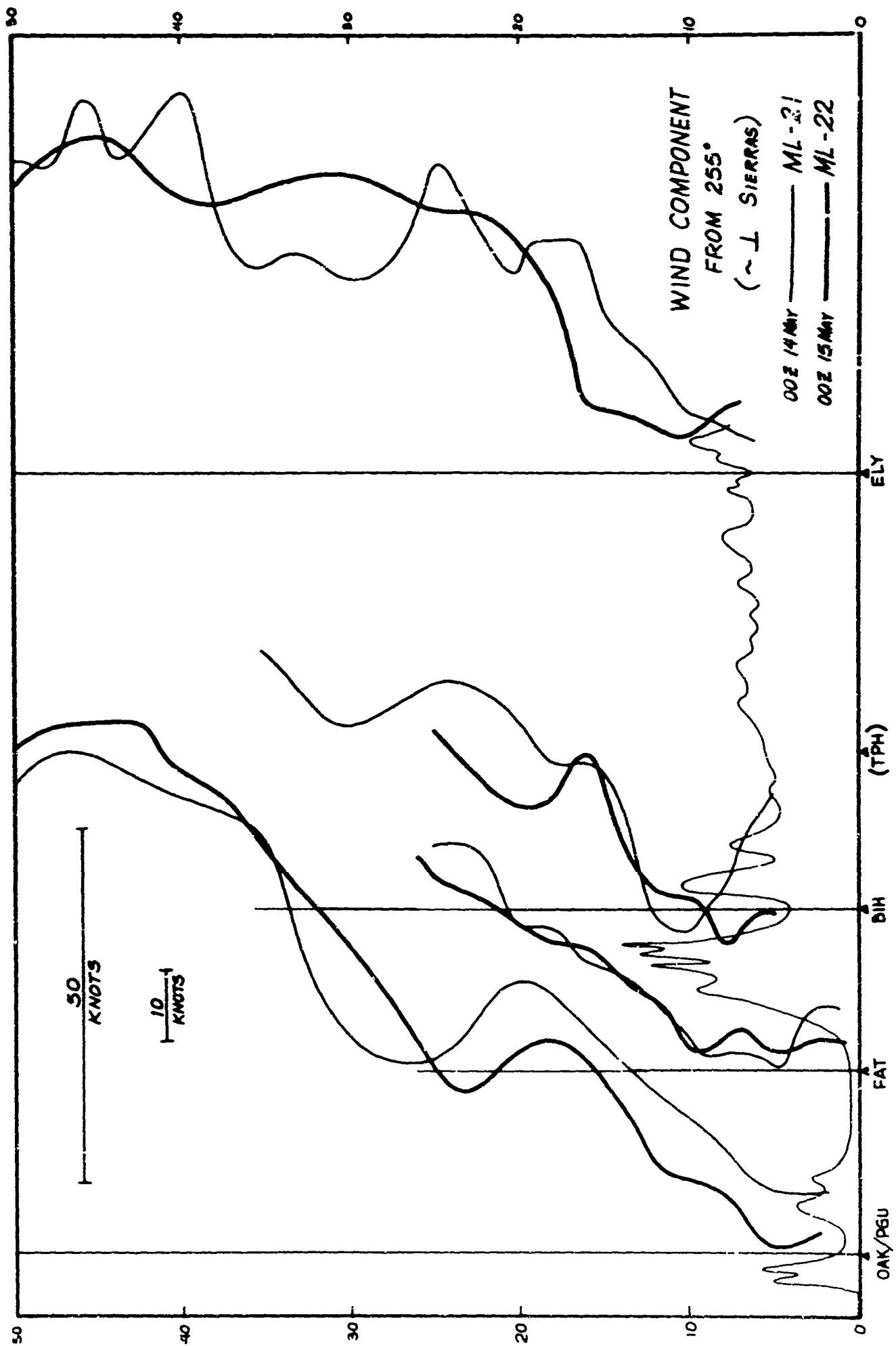
FIGURE 8.   Center diagram: Scorer number for upstream

interpolated profiles of wind and temperature.

Left and right diagrams: Terms contributing

to Scorer number.

Light lines, 00 GCT 14 May, 1964.

Heavy lines, 00 GCT 15 May, 1964.
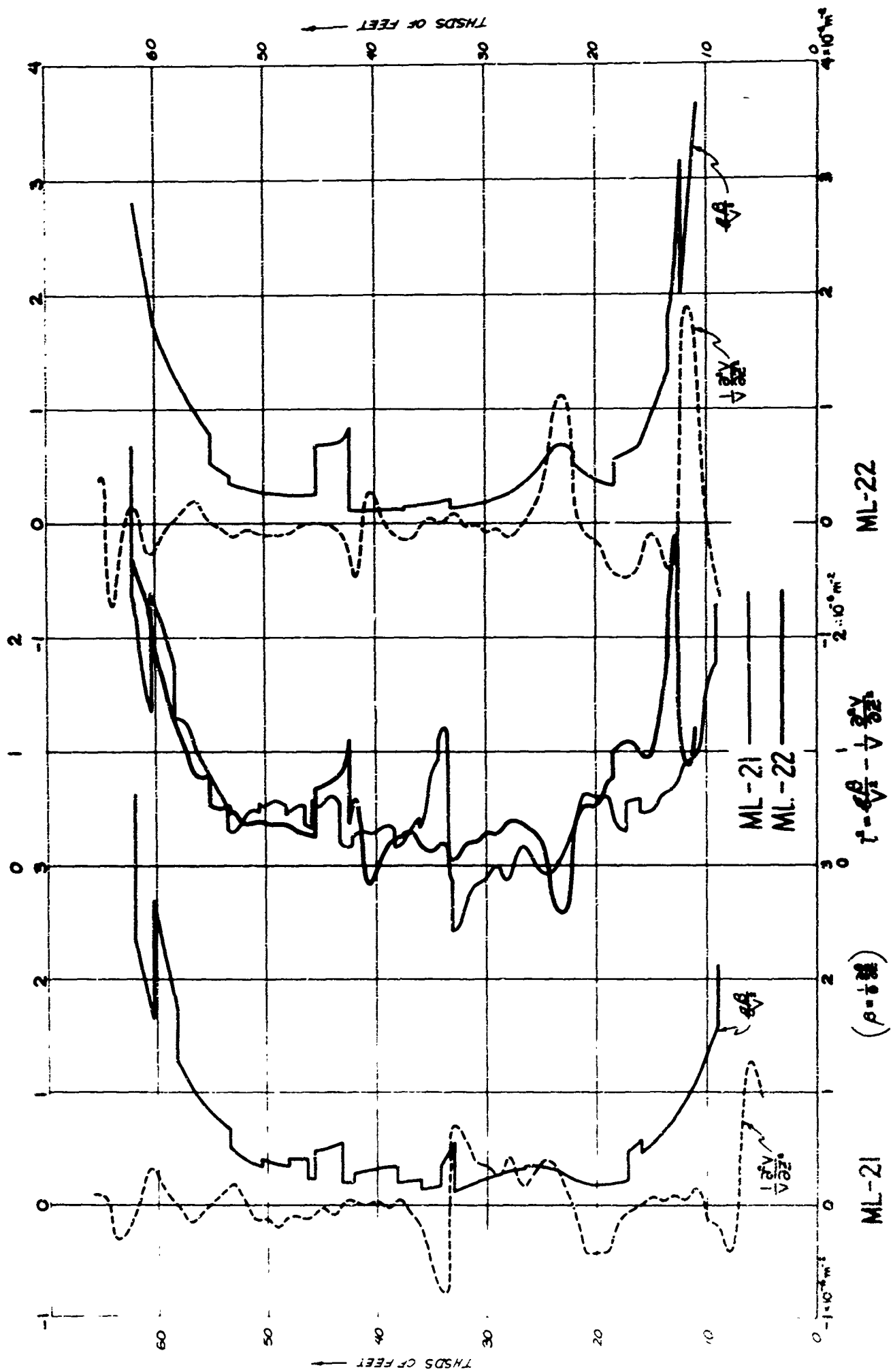
FIGURE 9.   U-2 wind direction soundings near FAT and TPH.

Large dots are soundings obtained during first set
of traverses.

Medium dots are soundings obtained during second
set of traverses (ML-21 only).

Small dots are for TPH descent sounding.

ML-21 FRA   ML-22 FRA   ML-21 TPH   ML-22 TPH

ALTITUDE IN THSDS OF FEET

60

50

40

240   260   240   260   220   240   260   220   240   260

U-2   WIND DIRECTION
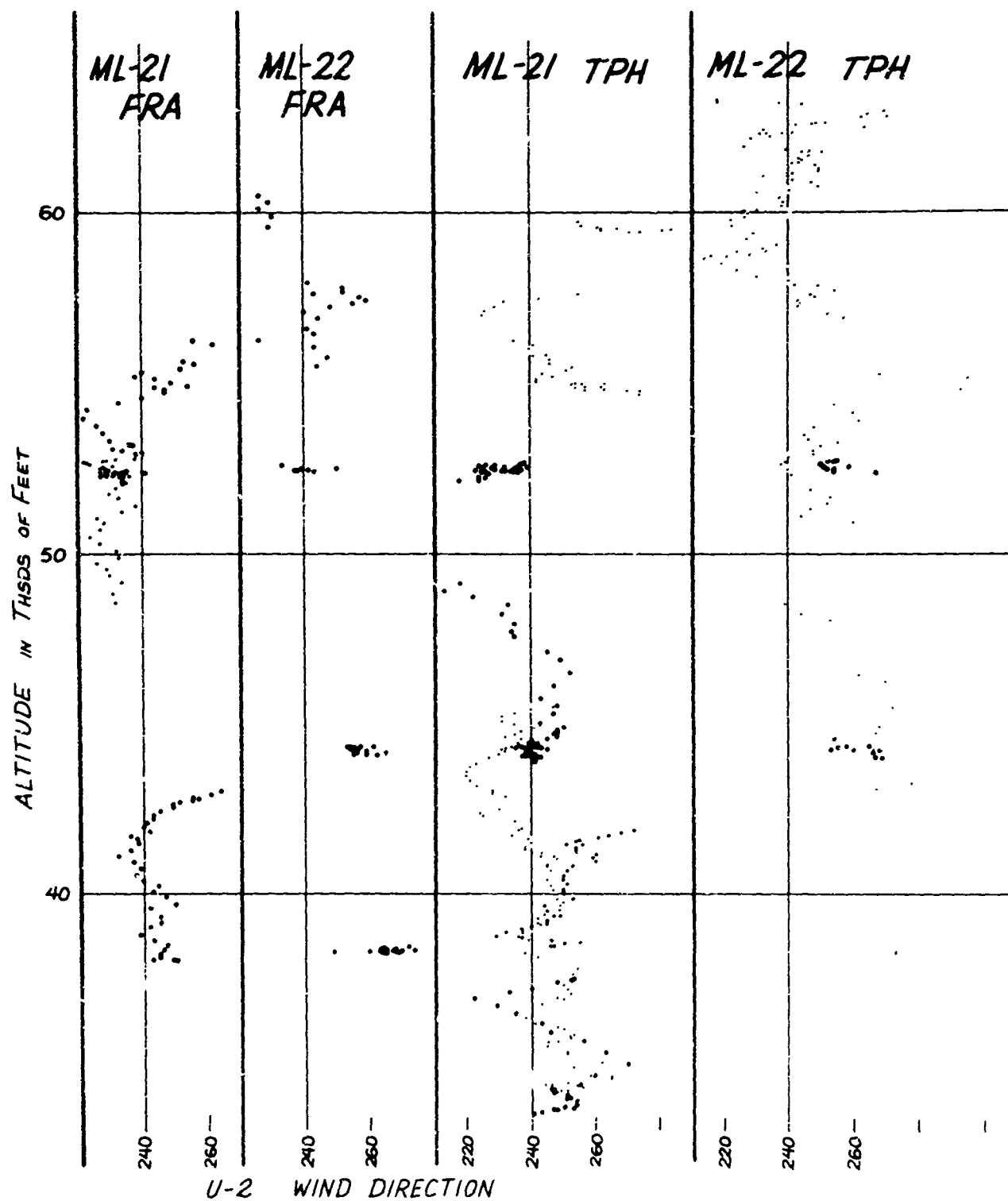
FIGURE 10.   U-2 wind speed soundings near FAT and TPH.

Dots same as preceding figure.

ML-21
FRA

ML-22
FRA

ML-21
TPH

ML-22
TPH

ALTITUDE IN THSDS OF FEET

60

50

40

20 40   40 60   20 40 60   20 40 60

U-2 WIND SPEED IN KNOTS
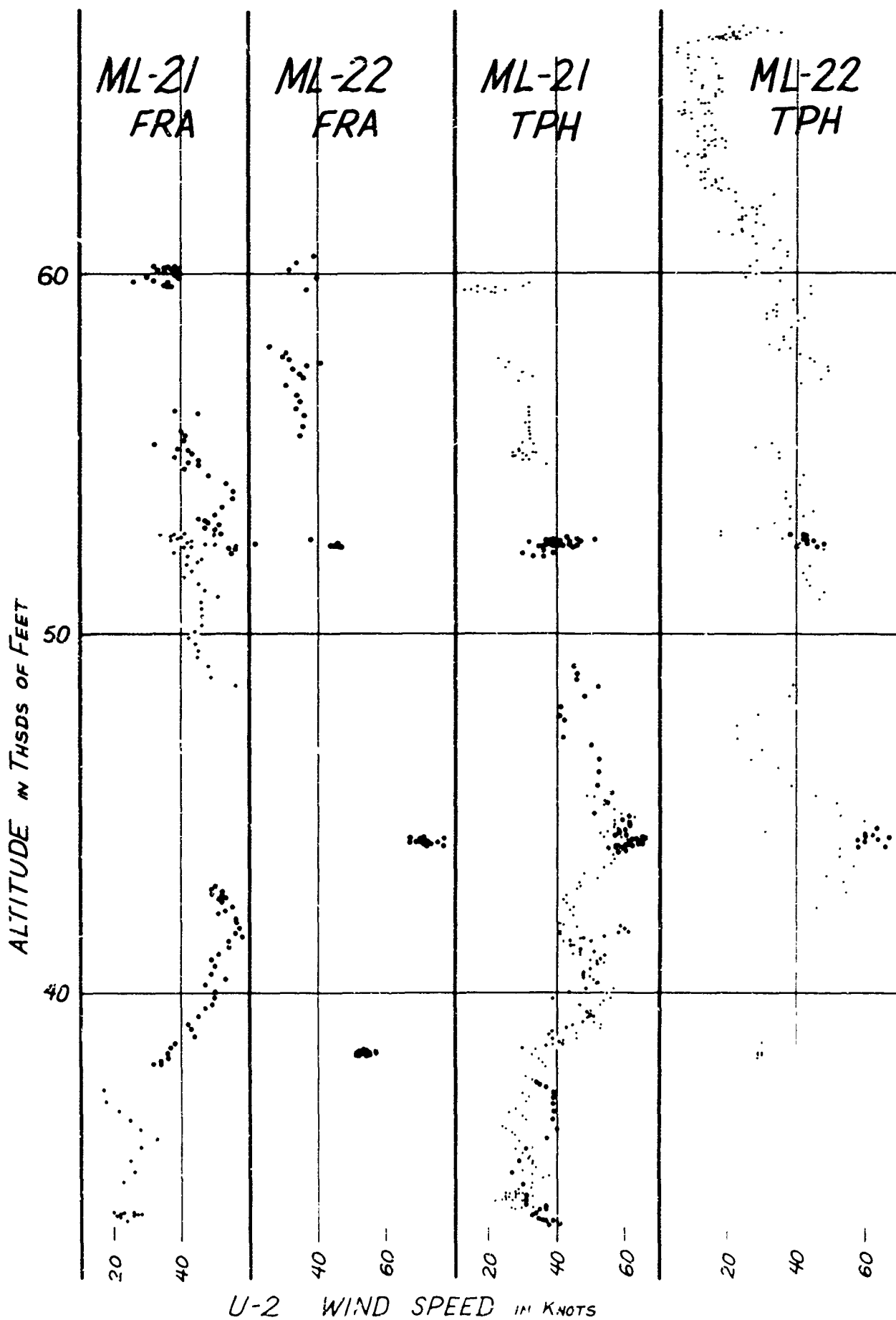
FIGURE 11.   U-2 temperature soundings near FAT and TPH.

Dots same as preceding figure.

ML-2/ FRA ML-22 FRA ML-2/ TPH ML-22 TPH

U-2 TEMPERATURES IN °C

ALTITUDE IN THSDS OF FEET
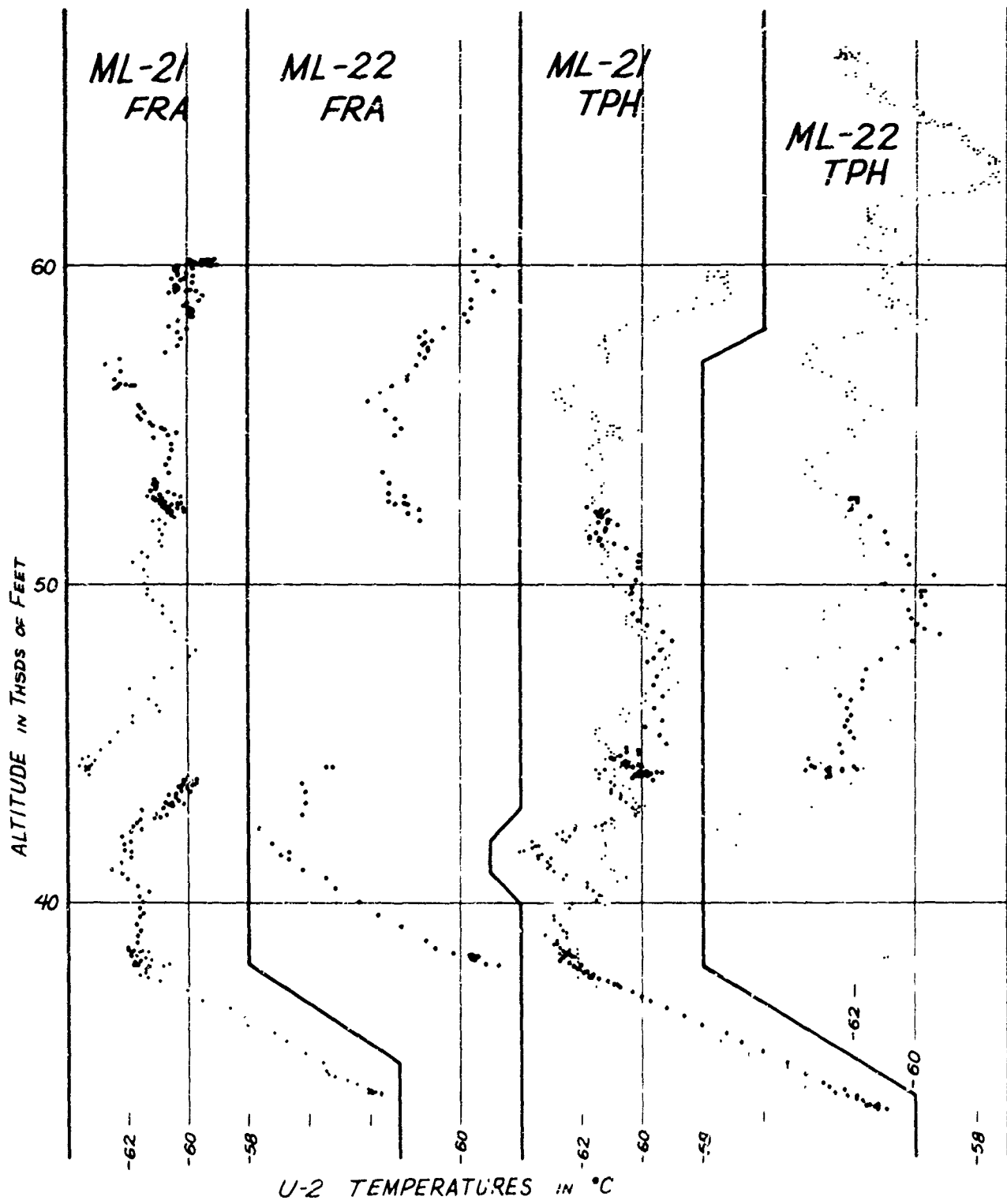
FIGURE 12.   Isentrope $\left(\Theta\right)$ analysis for first five ML-21

traverses.

ML-21

θ

SIERRA NEVADA MTS
OWENS VALLEY
WHITE MTS.

ALTITUDE IN THOUSANDS OF FEET
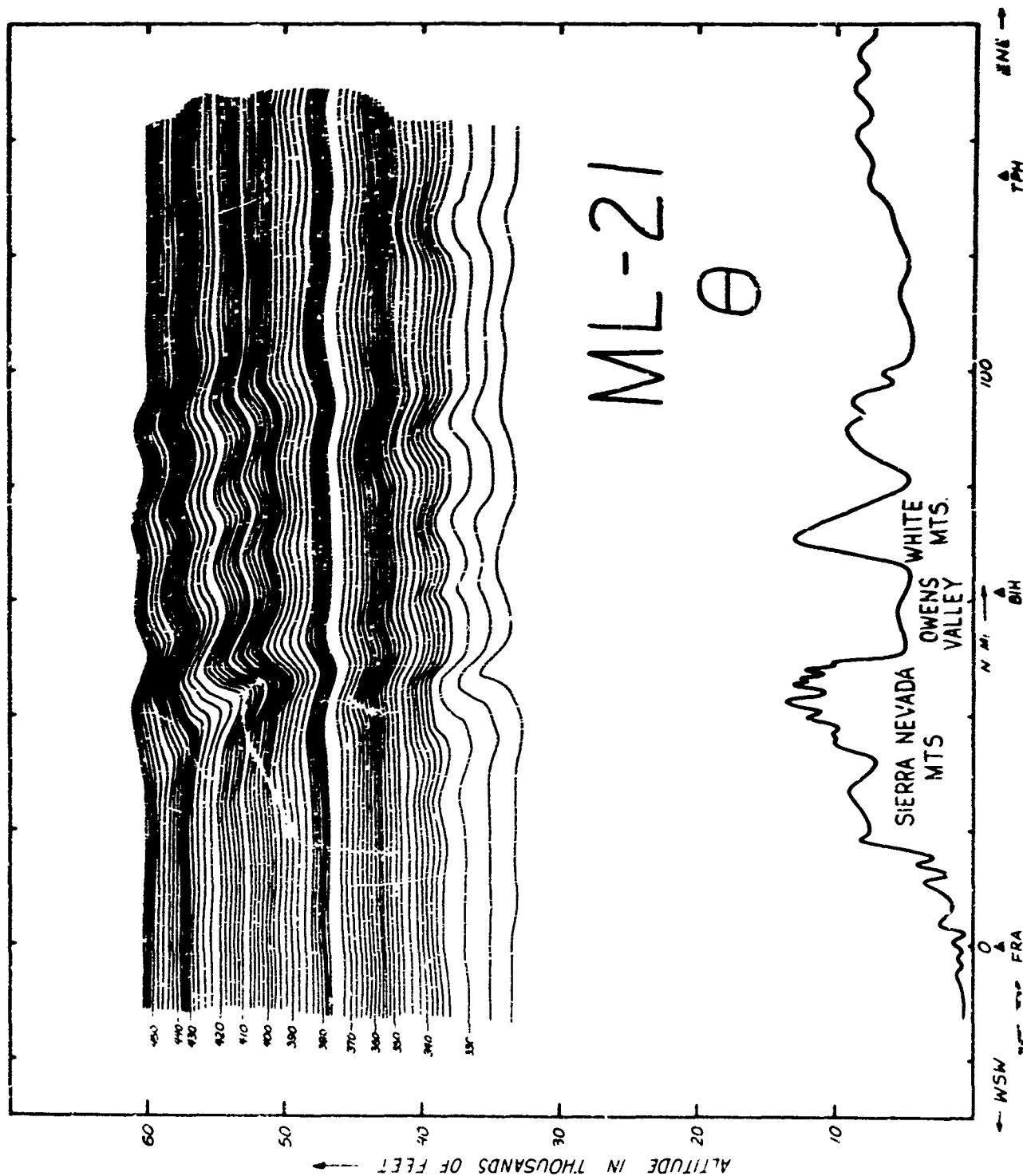
FIGURE 13a.   Isentrope height-departure $\left(\Delta Z_\theta\right)$ analysis

for first five ML-21 traverses.

Turbulence recorded at locations of zigzag lines.

Errata:

Figures 13a and 13b should be interchanged. The captions will then
refer to the proper diagram.

ML-21

ΔZ_o

X IN N MI ⟶

P-ALT IN FEET x 10³
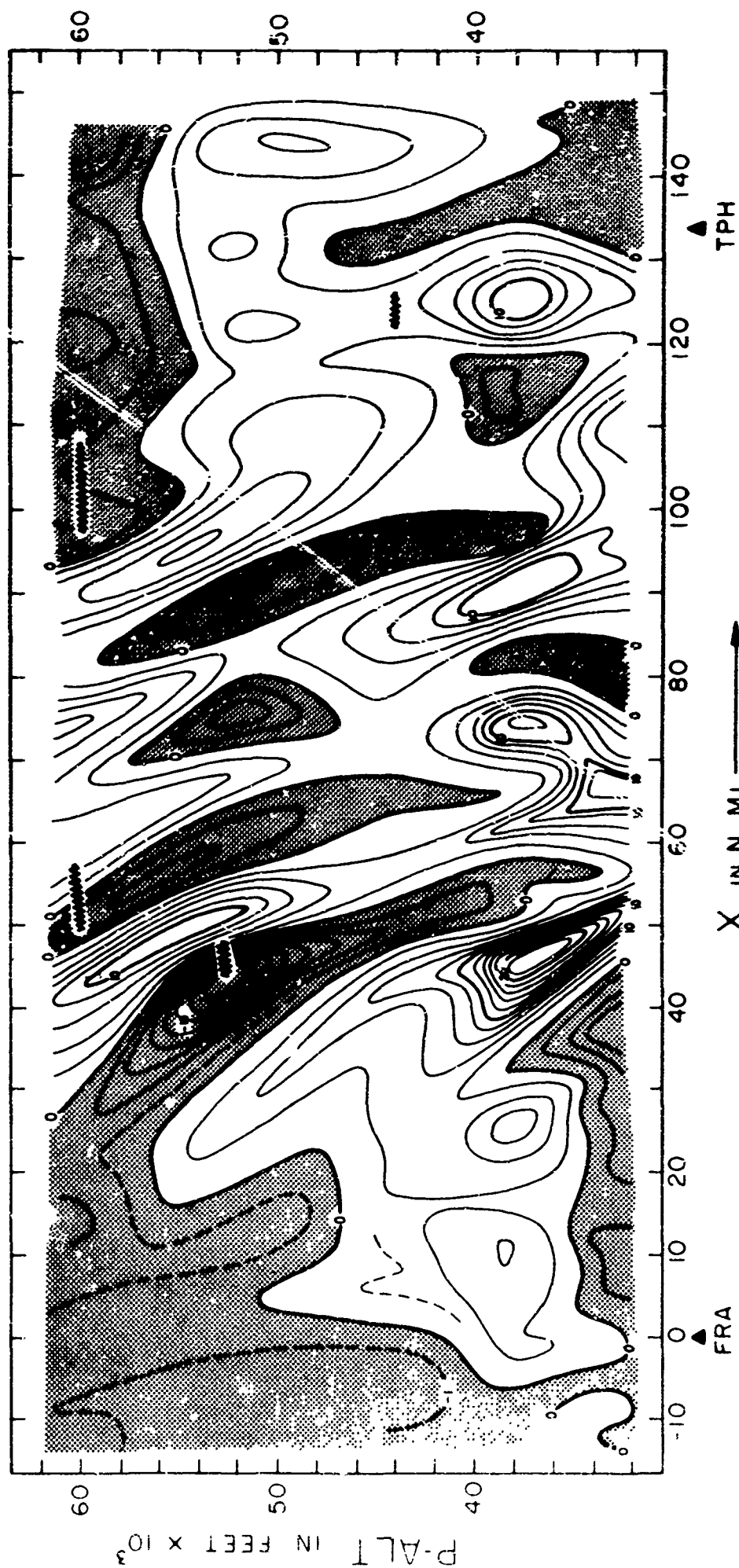
FIGURE 13b.   Same as Figure 13a, but repeated in format of

following Figures for comparison purposes.

ML-21

ΔZ_θ

SIERRA NEVADA
MTS

OWENS
VALLEY

WHITE
MTS

ALTITUDE IN THOUSANDS OF FEET
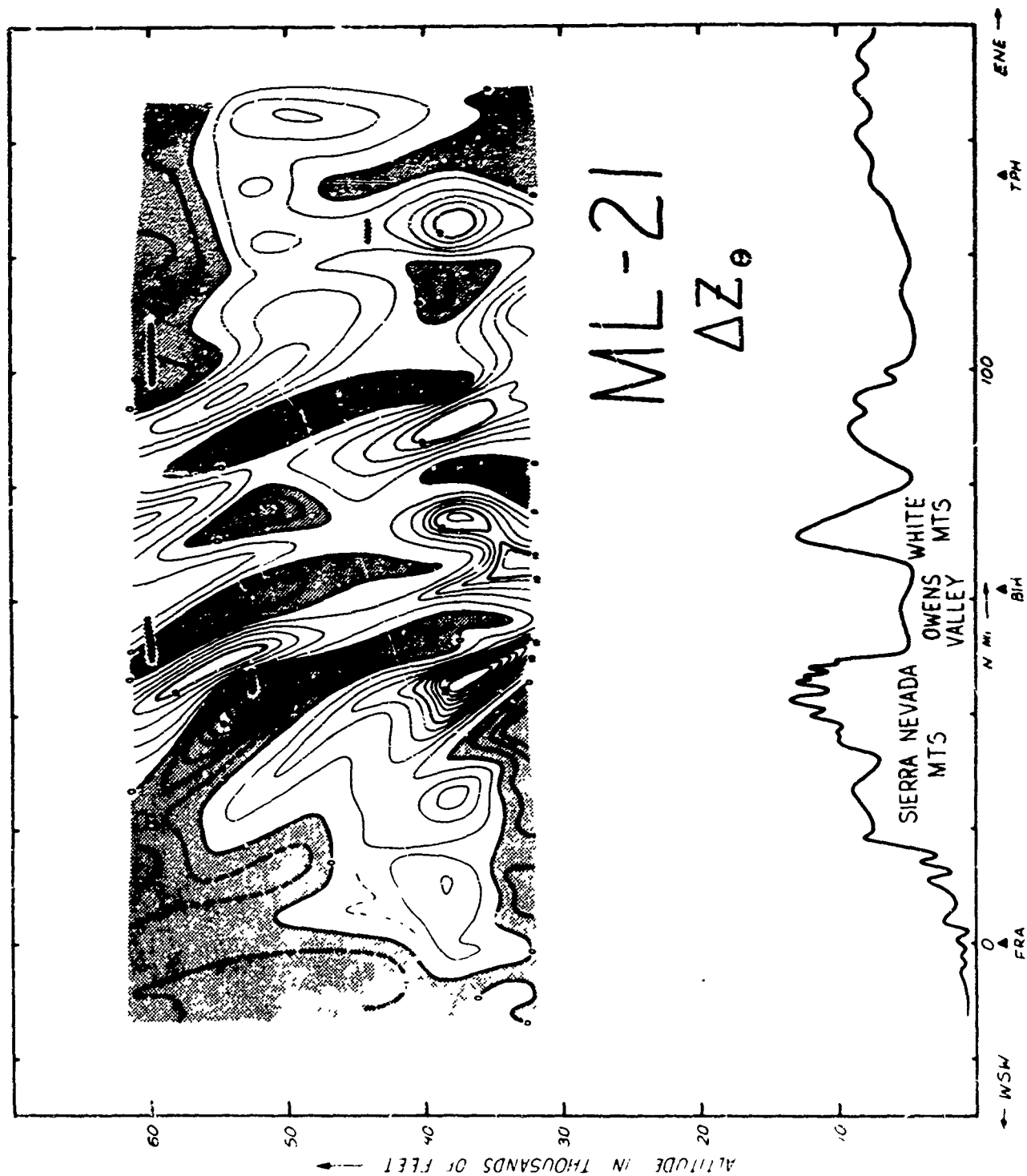
FIGURE 14.   Wind-speed ratio $\left(\dfrac{u}{\overline{u}_L}\right)$ analysis for first

five ML-21 traverses.

ML-21

$$\frac{U}{U_L}\left(\approx \frac{U}{U_r}\right)$$

X IN N MI →
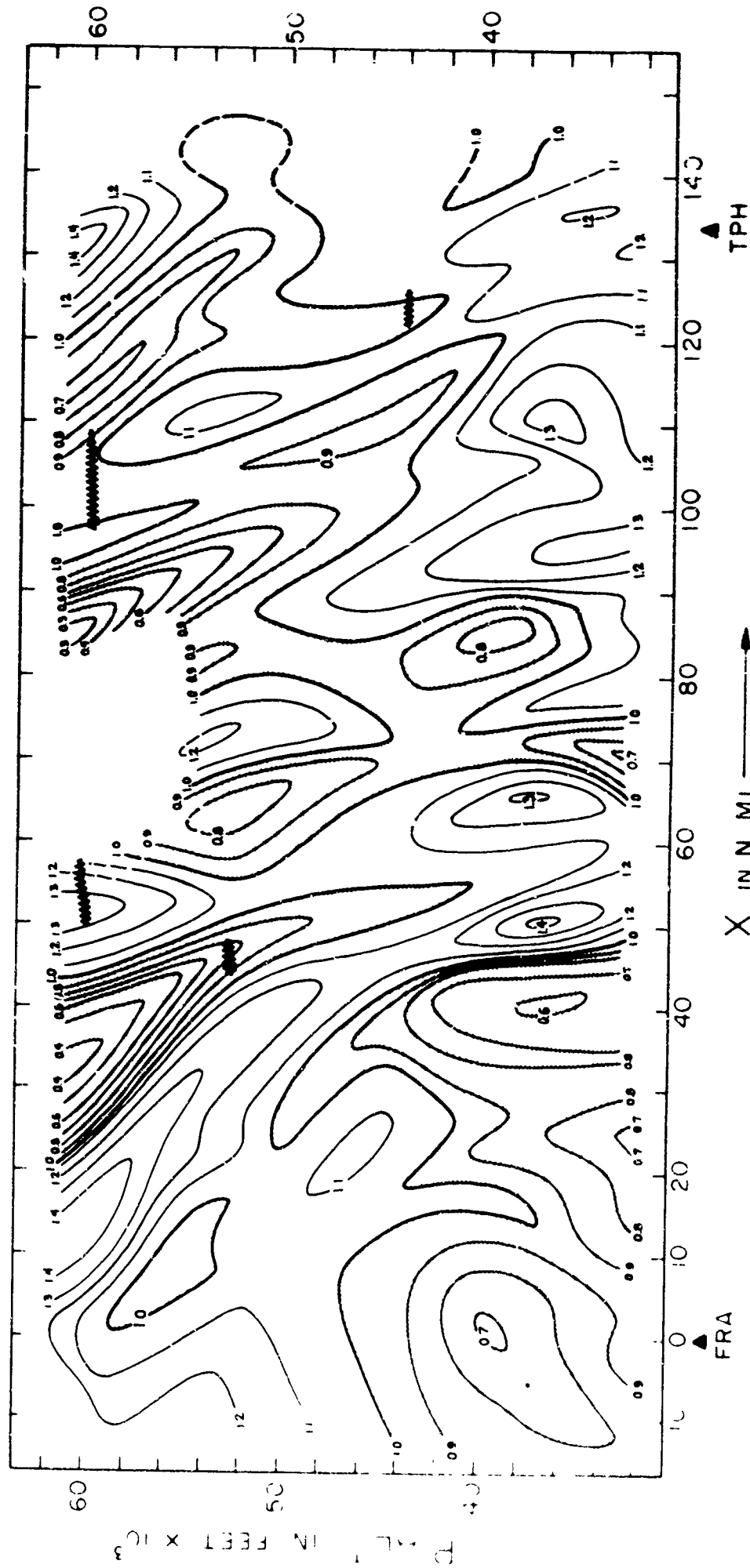
FIGURE 15. $1 - \dfrac{\delta(\Delta z_{\bullet})}{\delta z}$ analysis for first five

ML-21 traverses.

Turbulence recorded at locations of zigzag lines.

ML-21

$1 - \dfrac{\delta(\Delta z_o)}{\delta z}$
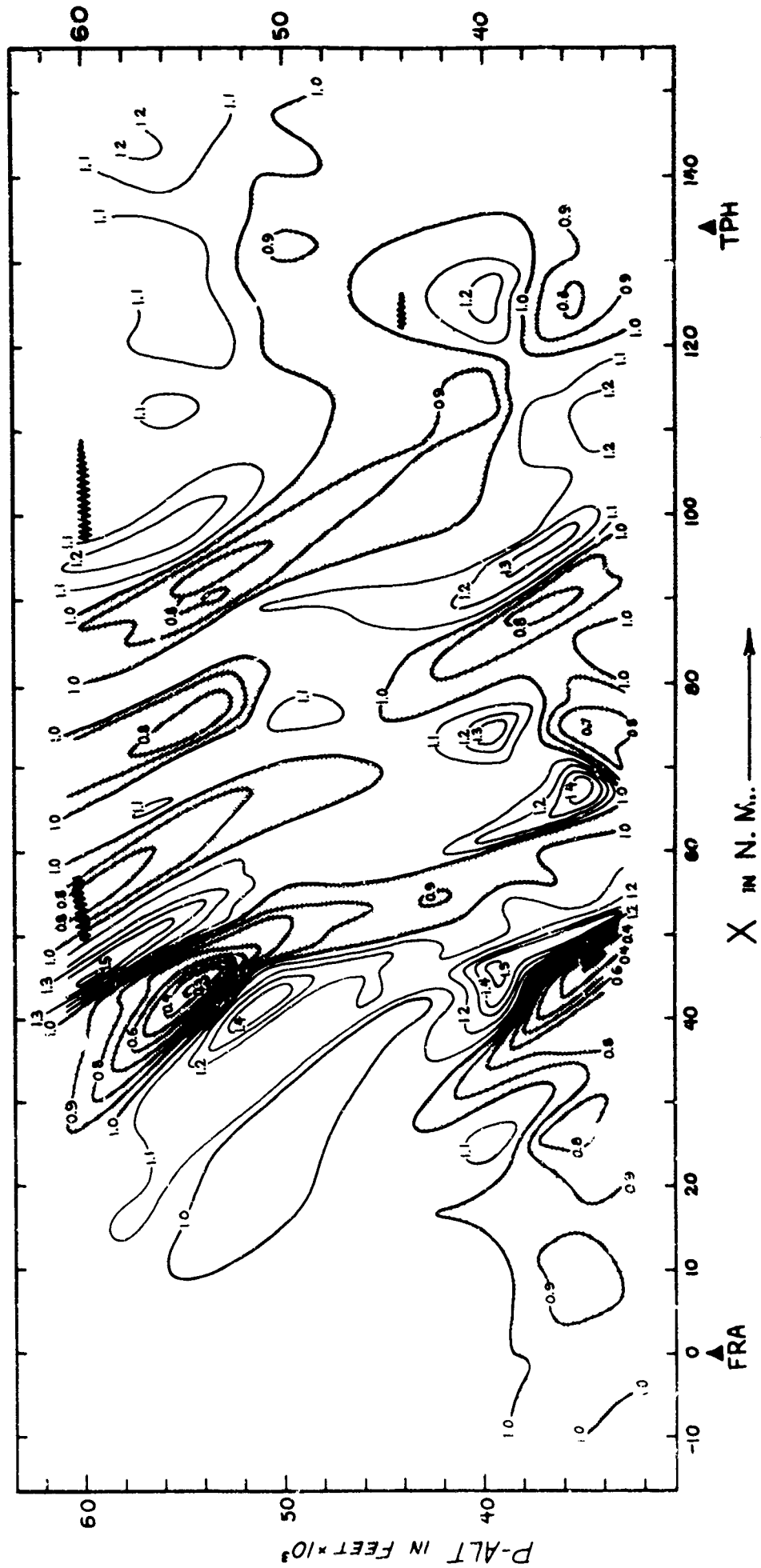
FIGURE 16.   Superimposition of Figures 14 and 15.

Horizontal hatching where $\frac{u}{u_i} < 1$

Vertical hatching where $1 - \frac{\delta(\Delta z_e)}{\delta z} < 1$

$$\text{COMPARISON } \frac{u}{u_c} \text{ AND } 1 - \frac{\delta(\Delta z)}{\delta z} \quad ML\text{-}21$$

X IN N MI

ALT IN FEET × 10³

FRA TPH

60 50 40

60 50 40
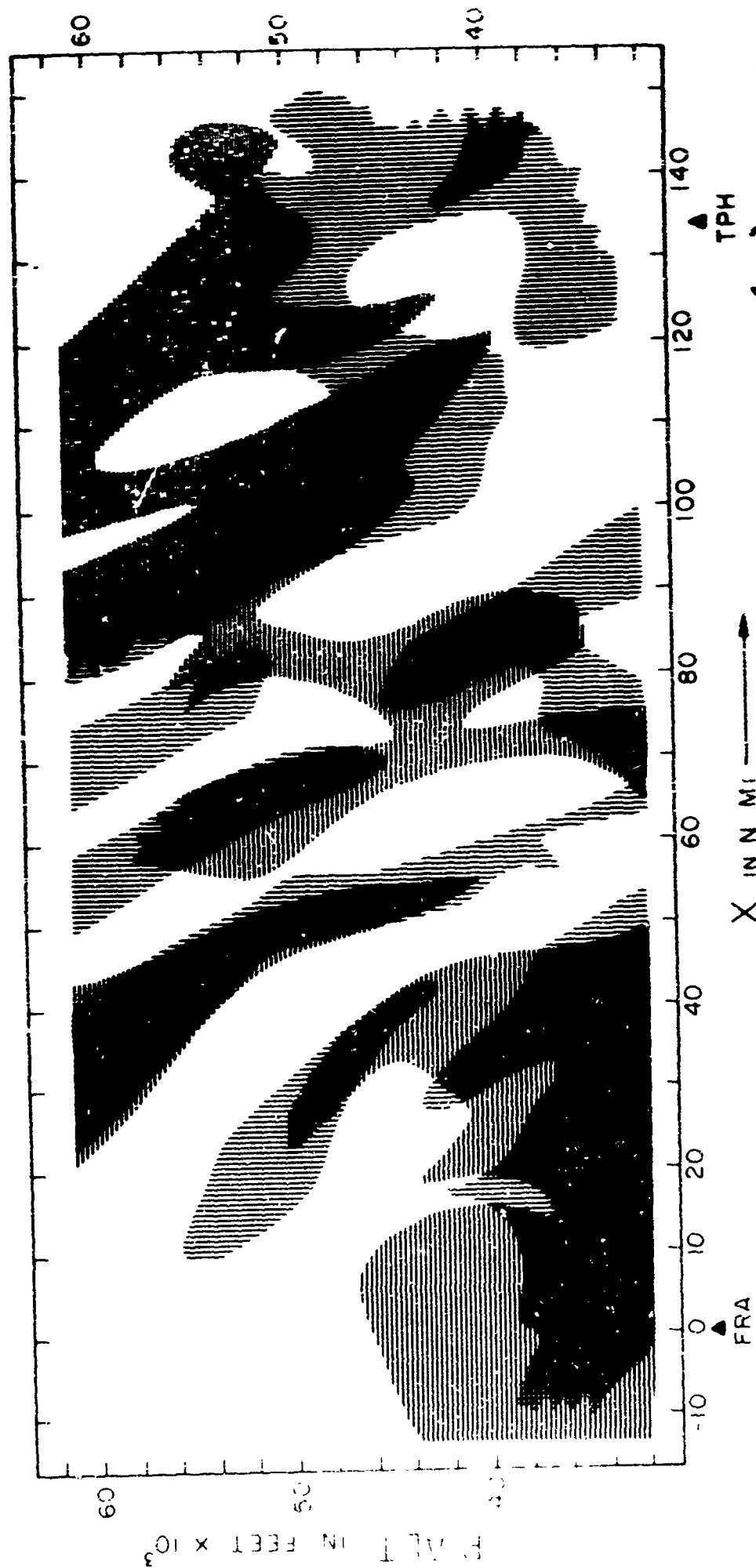
FIGURE 17.   Graphs of U-2 data for ML-21 traverses 1 (solid)

and 6 (dashed) from 60-second mean data.

ML-21
~34,000'
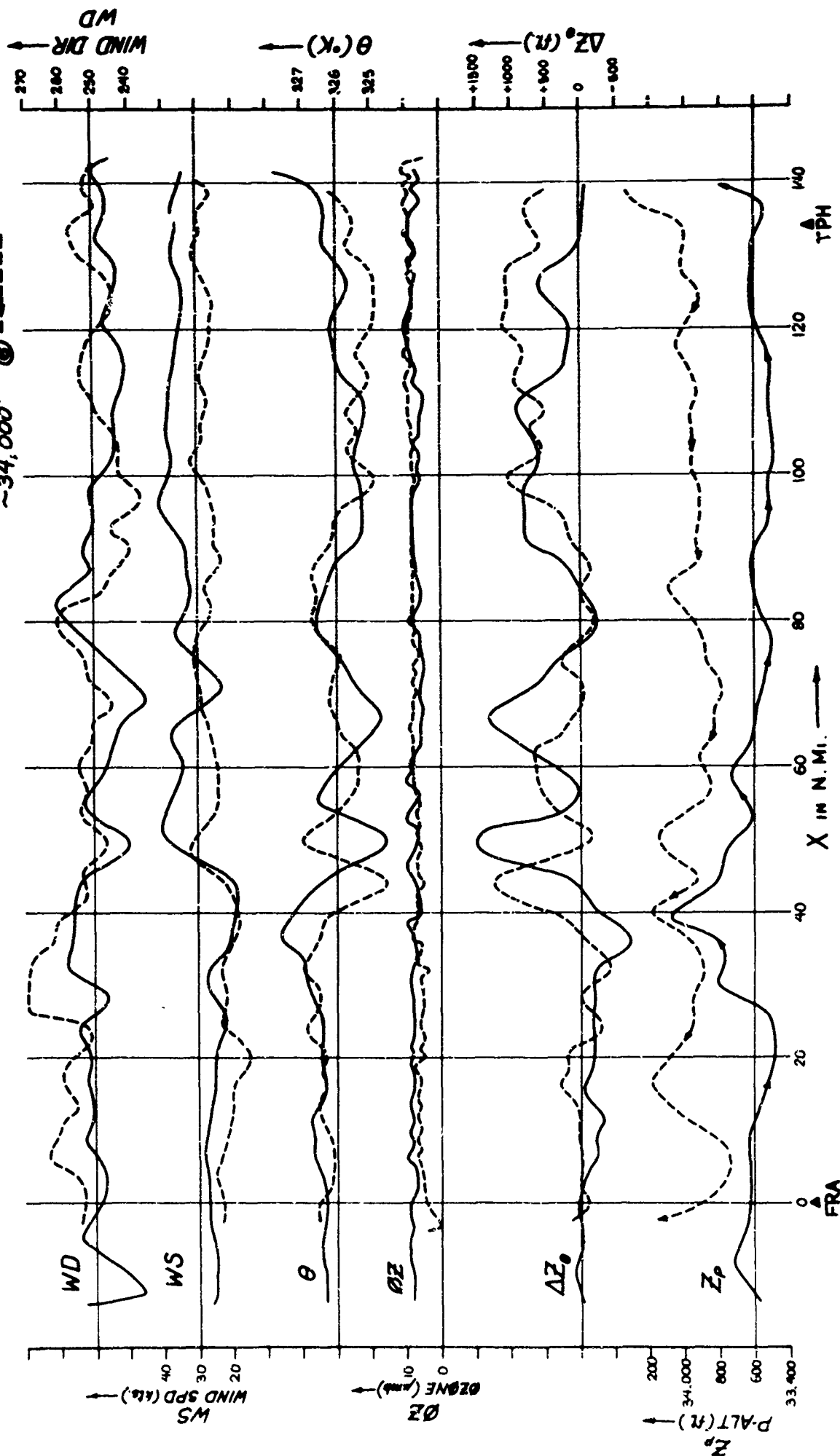
FIGURE 18.   Graphs of U-2 data for ML-21 traverses 2 (solid)

and 7 (dashed) from 60-second mean data.
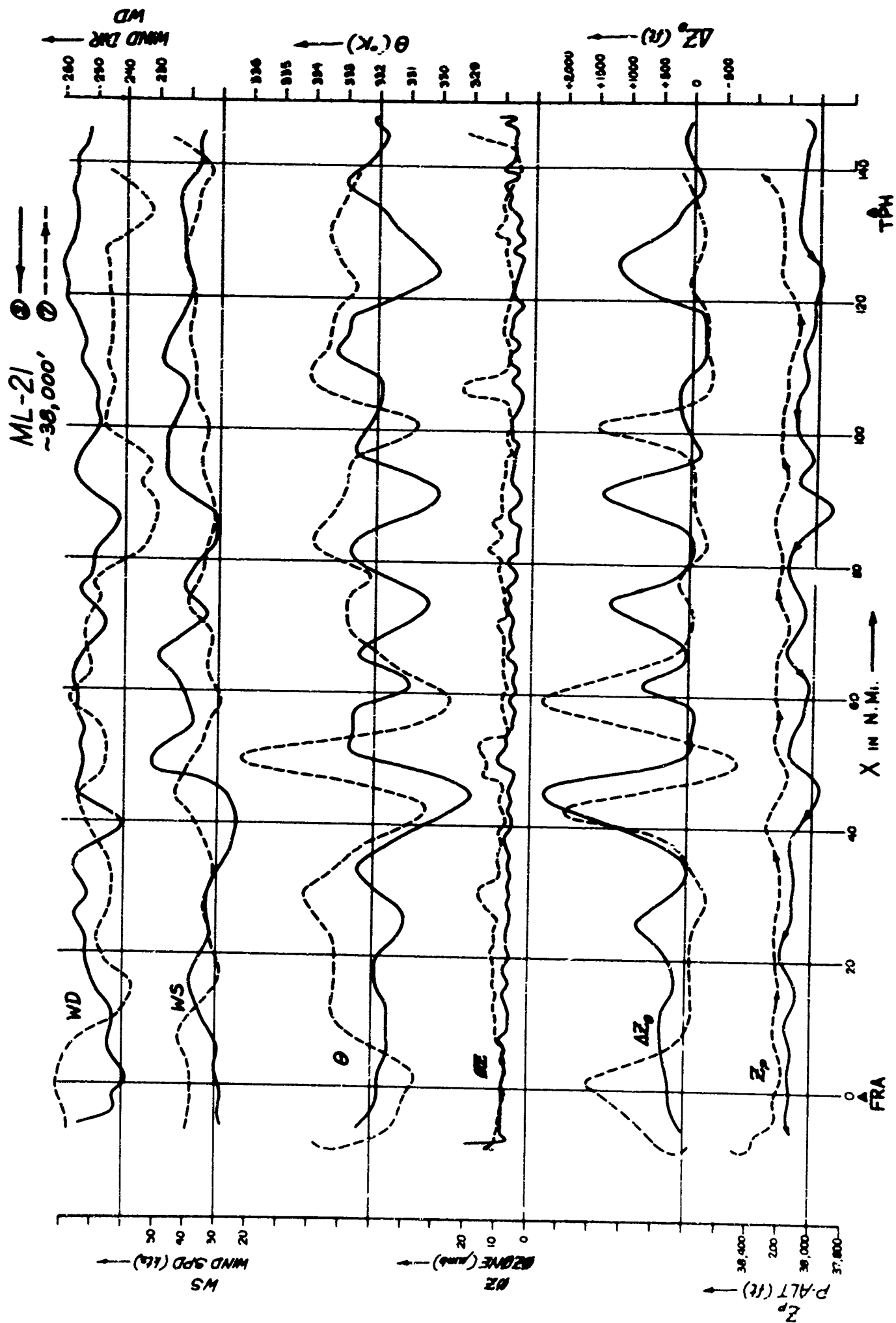
ML-21
~38,000'

FIGURE 19.   Graphs of U-2 data for ML-21 traverses 3 (solid) and 8 (dashed) from 60-second mean data.
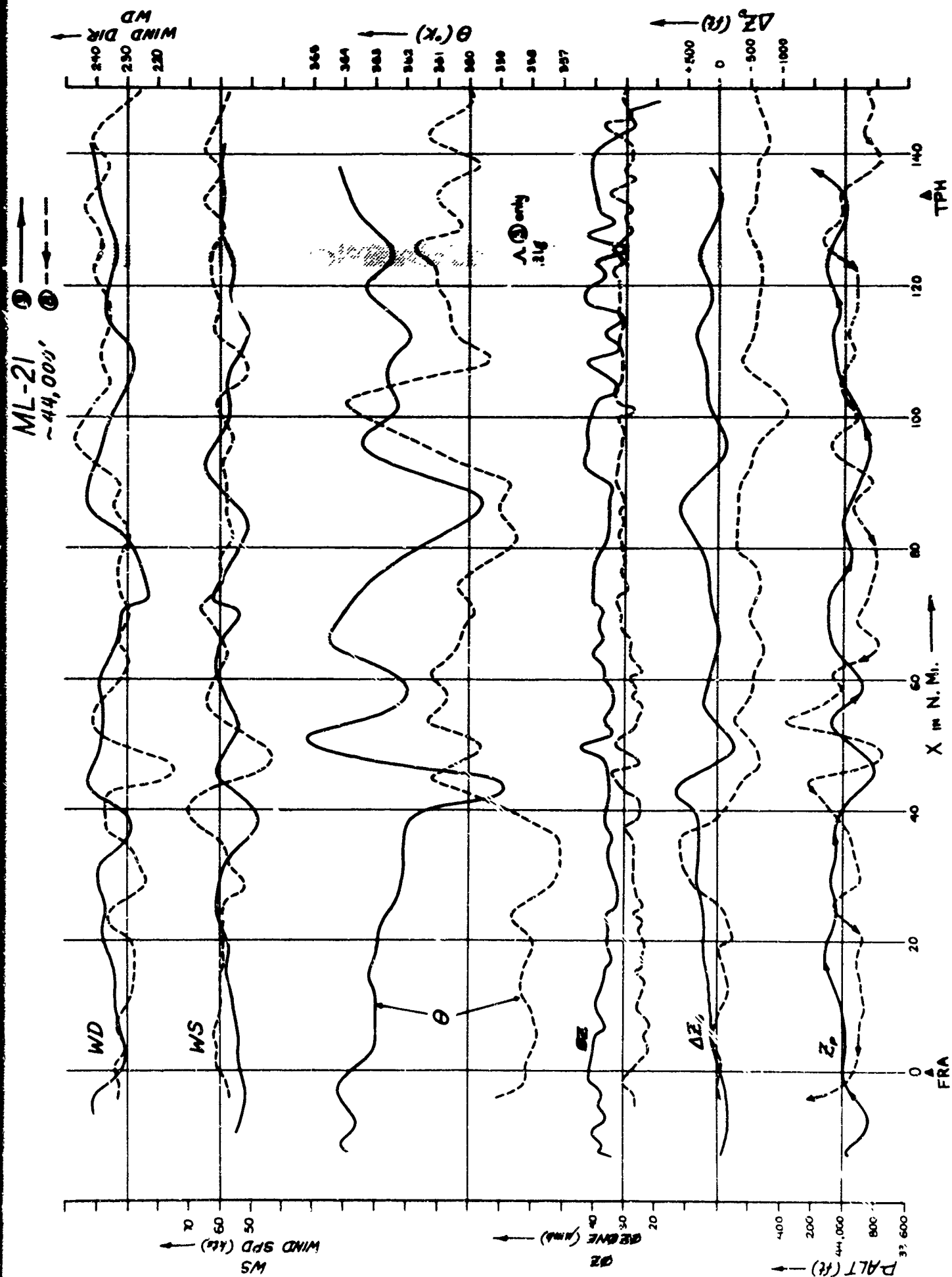
ML-21
~44,000'

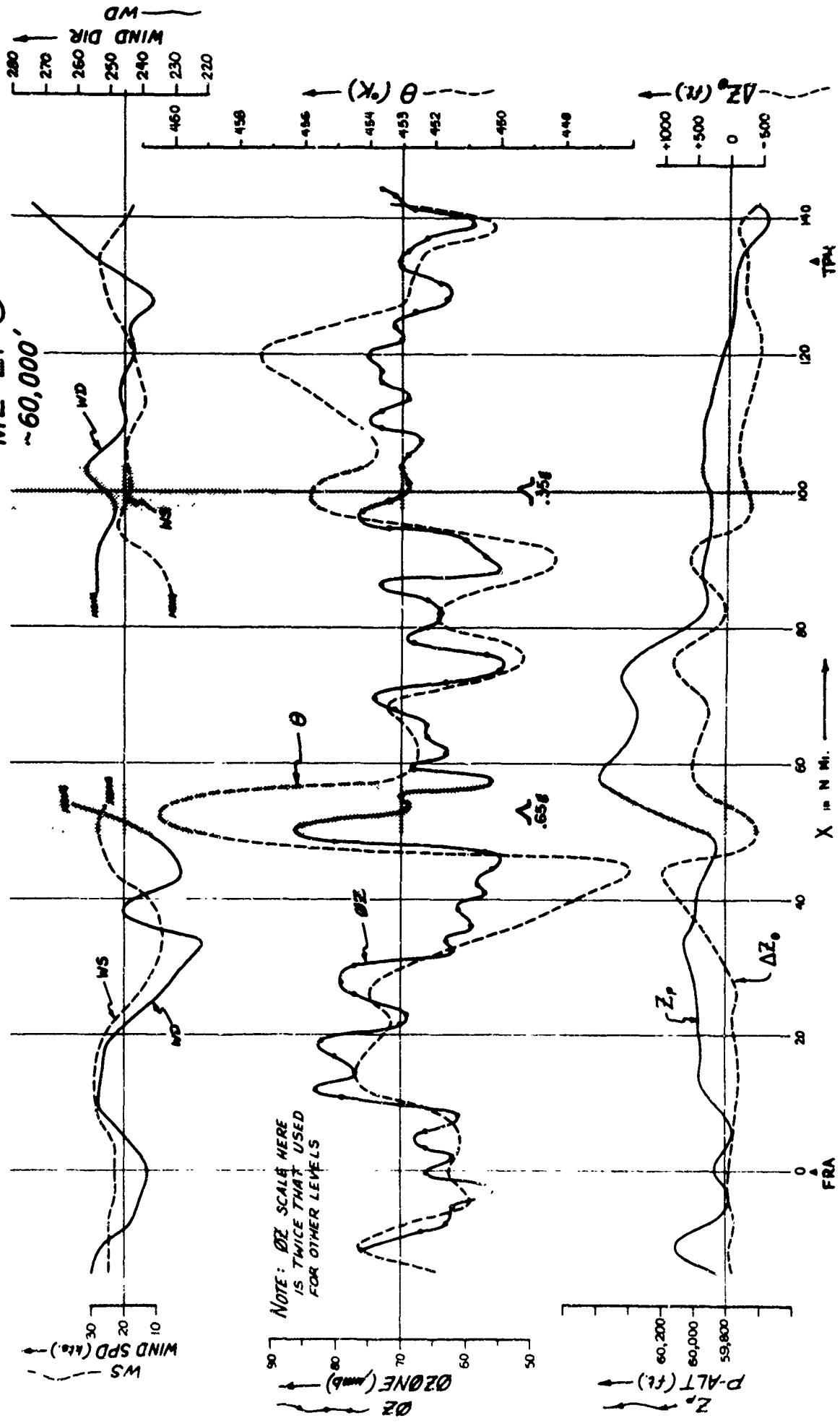FIGURE 20.   Graphs of U-2 dcta for ML-21 traverse 4,

from 60-second mean data.
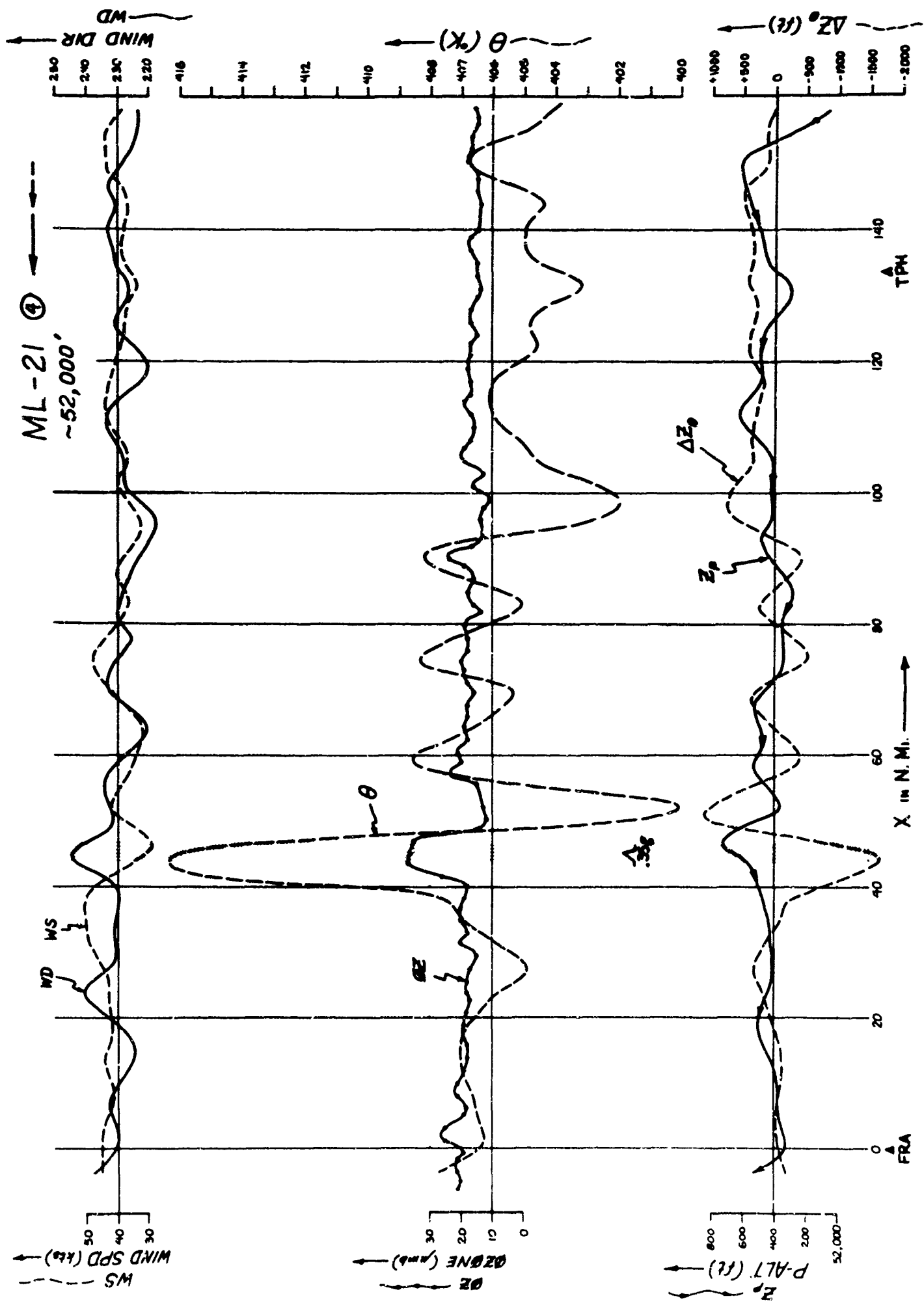
FIGURE 21.   Graphs of U-2 data for ML-21 traverse 5,
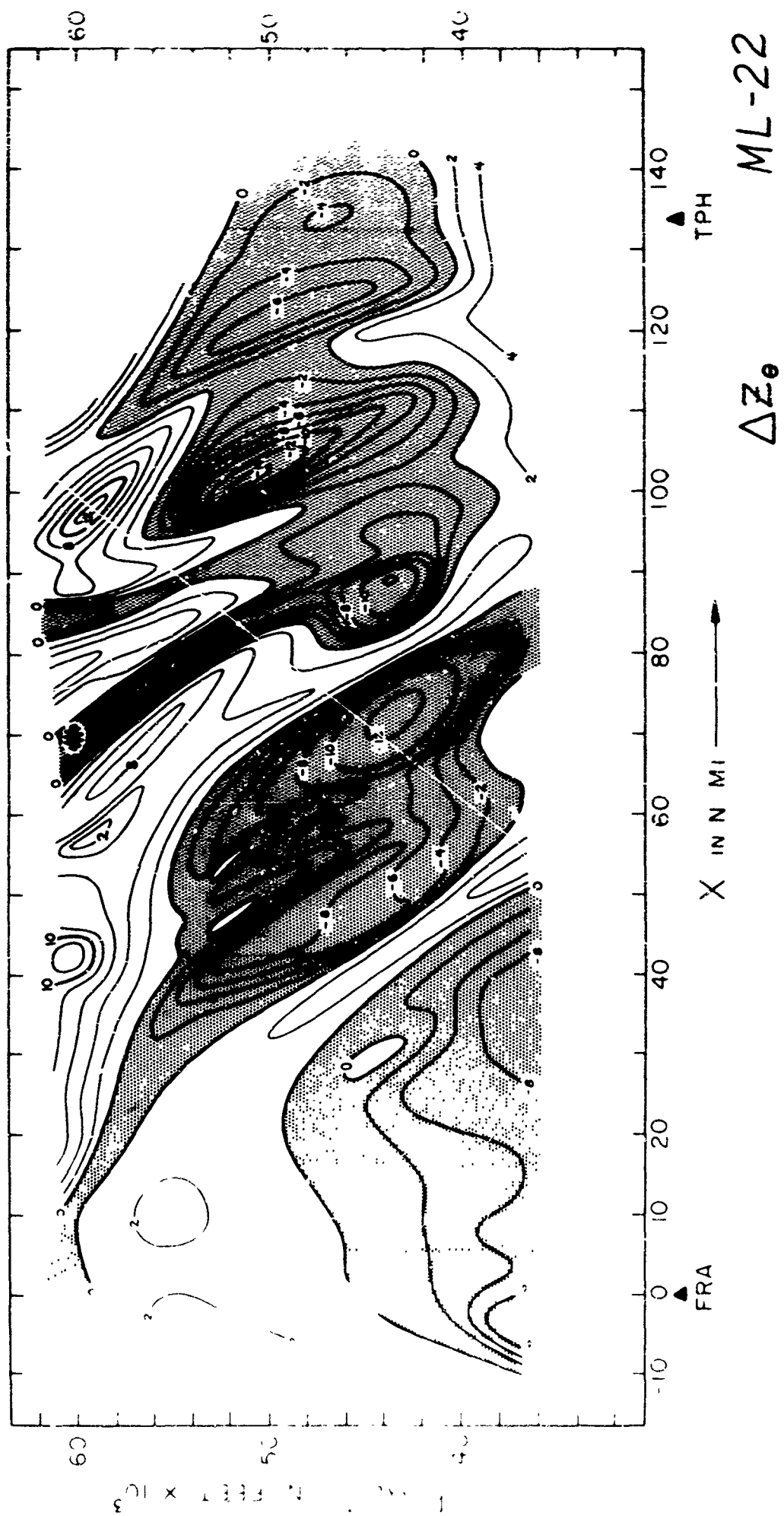
from 60-second mean data.

ML-21 ⑤ ~60,000'

FIGURE 22.   Isentrope height-departure $\left(\Delta Z_\theta\right)$ analysis
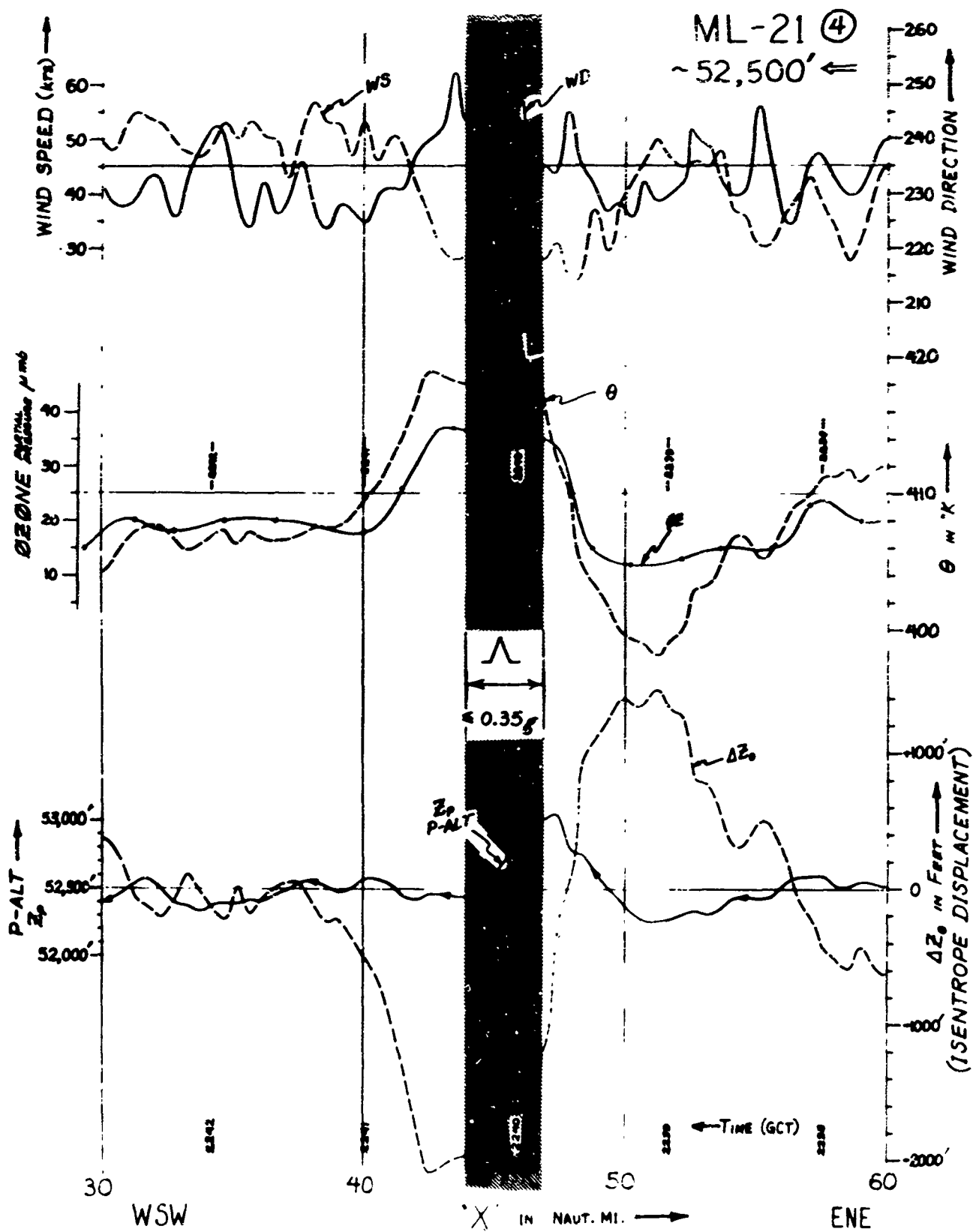
for ML-22 traverses.

ΔZ_θ ML-22

X IN N MI ———

FIGURE 23.   Horizontal temperature analysis at 60,000 feet

MSL for ML-22.

Turbulence recorded at locations marked by large

dots.

TURBULENCE:

	PREP	ACCEL
2118		.55
2130	√	.64
2206	√	
2210		.30

ANALYSIS OF
~60,500' TEMPERATURES

ML – 22

FIGURE 24.   Graphs of U-2 data for a portion of ML-21

traverse 4, from 5-second data.

FIGURE 25.   Graphs of U-2 data for a portion of ML-21
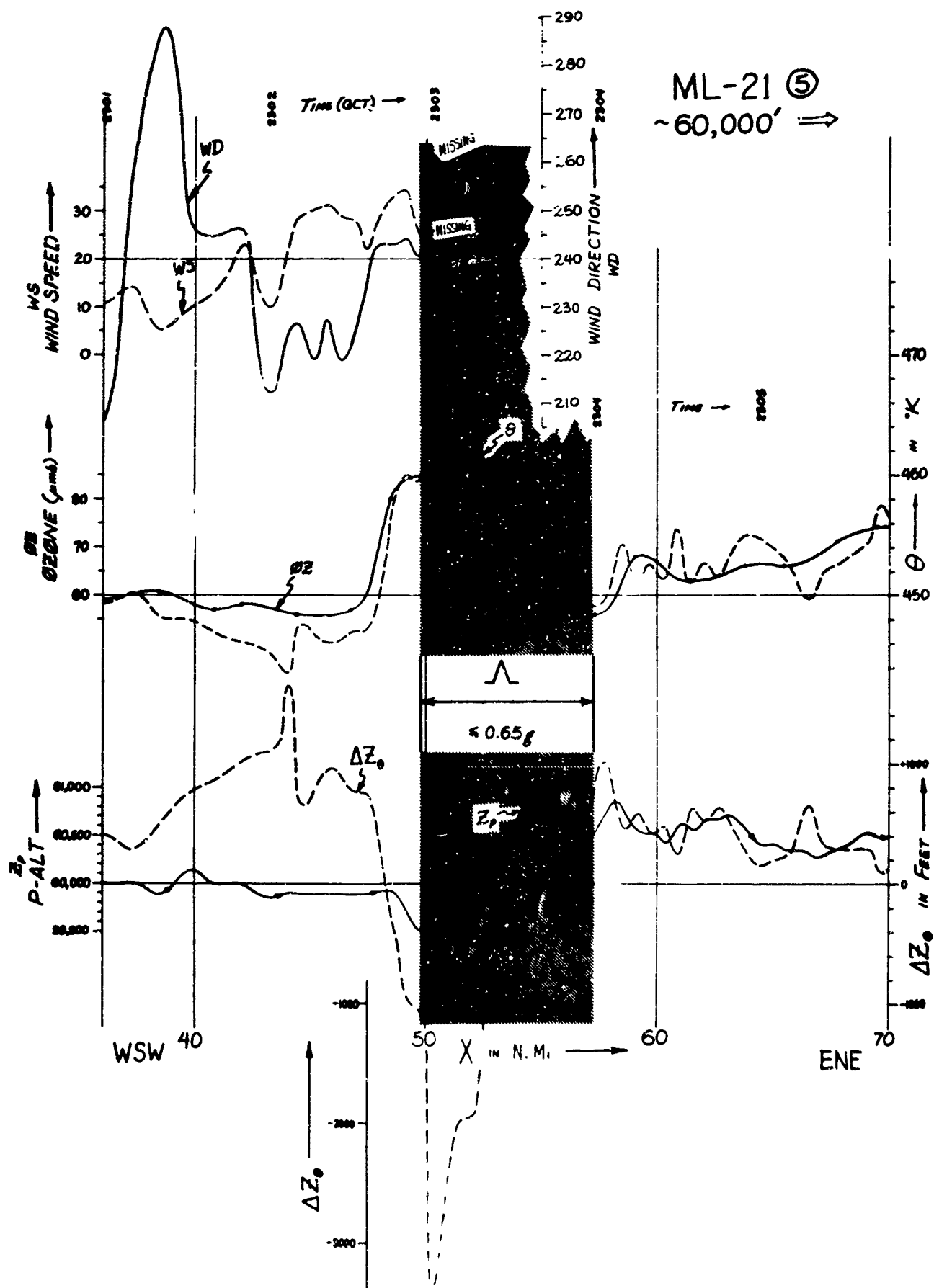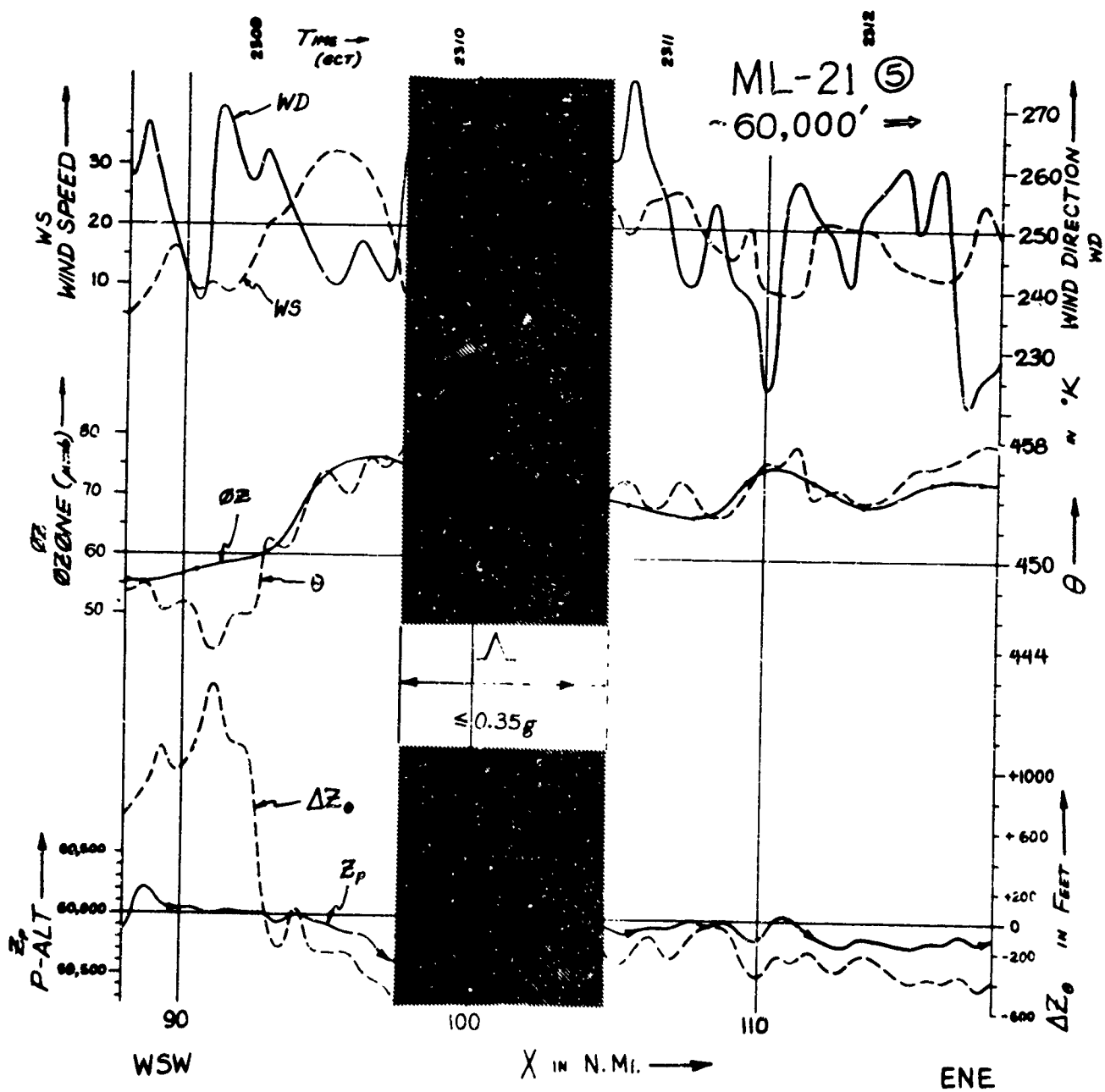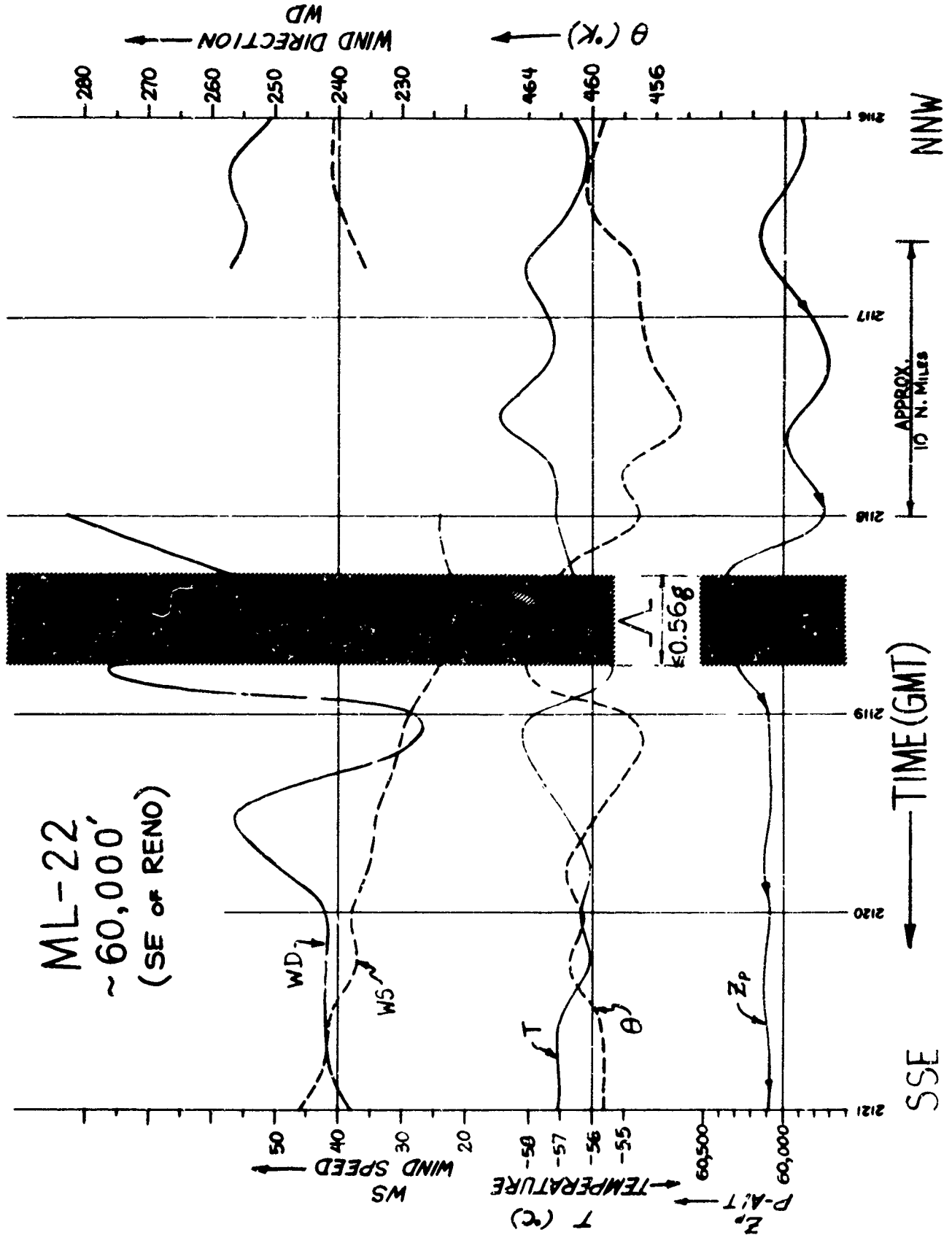
traverse 5, from 5-second data.

ML-21 ⑤
~60,000' ⟹

FIGURE 26.   Graphs of U-2 data for a somewhat later portion

of ML-21 traverse 5, from 5-second data.

ML-21 ⑤
~60,000' ⟹

FIGURE 27.   Graphs of U-2 data for a portion of ML-22

flight at 60,000 feet, near Reno, from 5-second

data.

ML-22
~60,000'
(SE of RENO)

FIGURE 28.   Graphs of U-2 data for a portion of ML-22 flight

at 60,000 feet, near Mono Lake, from 5-second

data.

ML-22
~60,000'
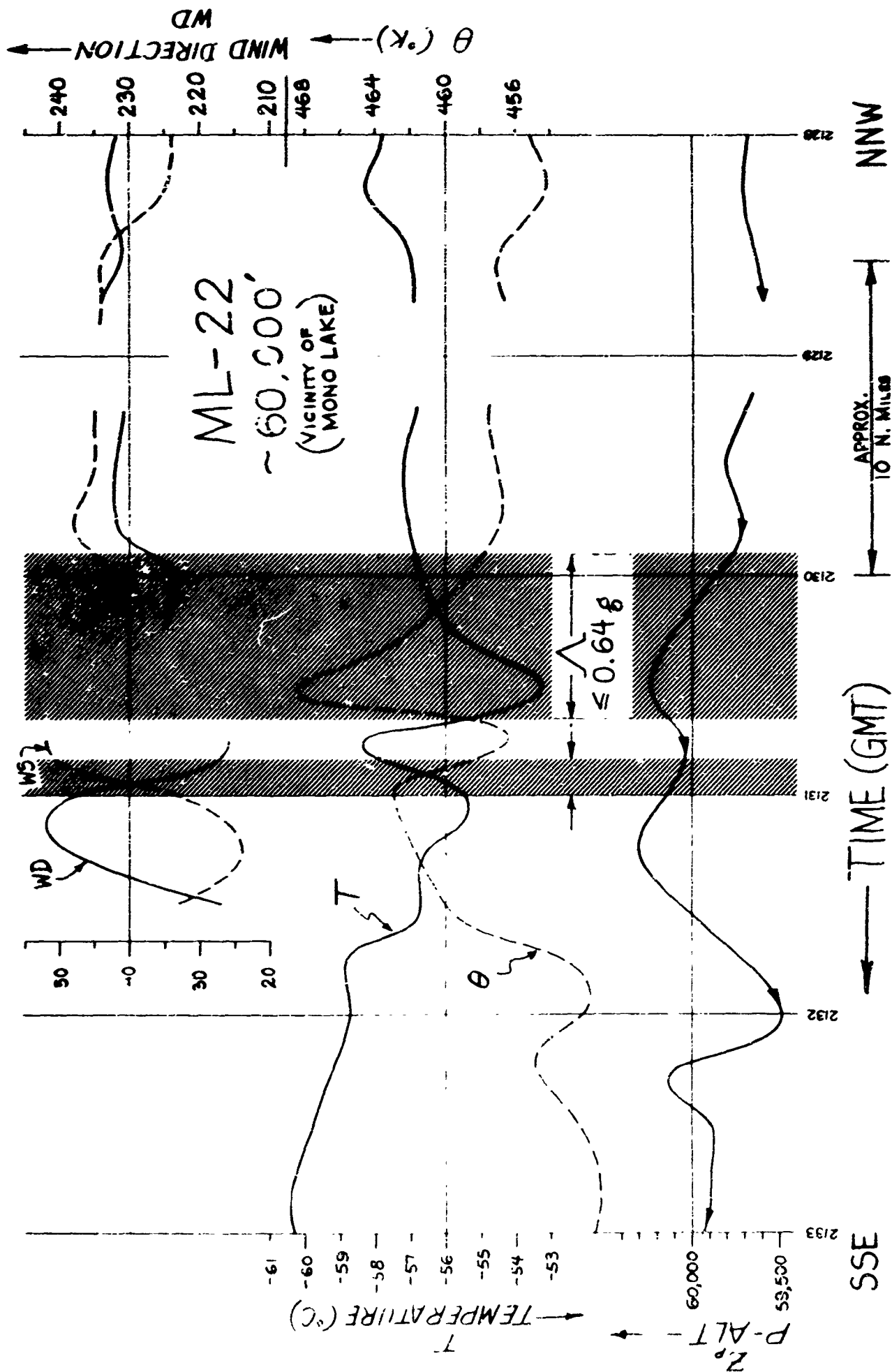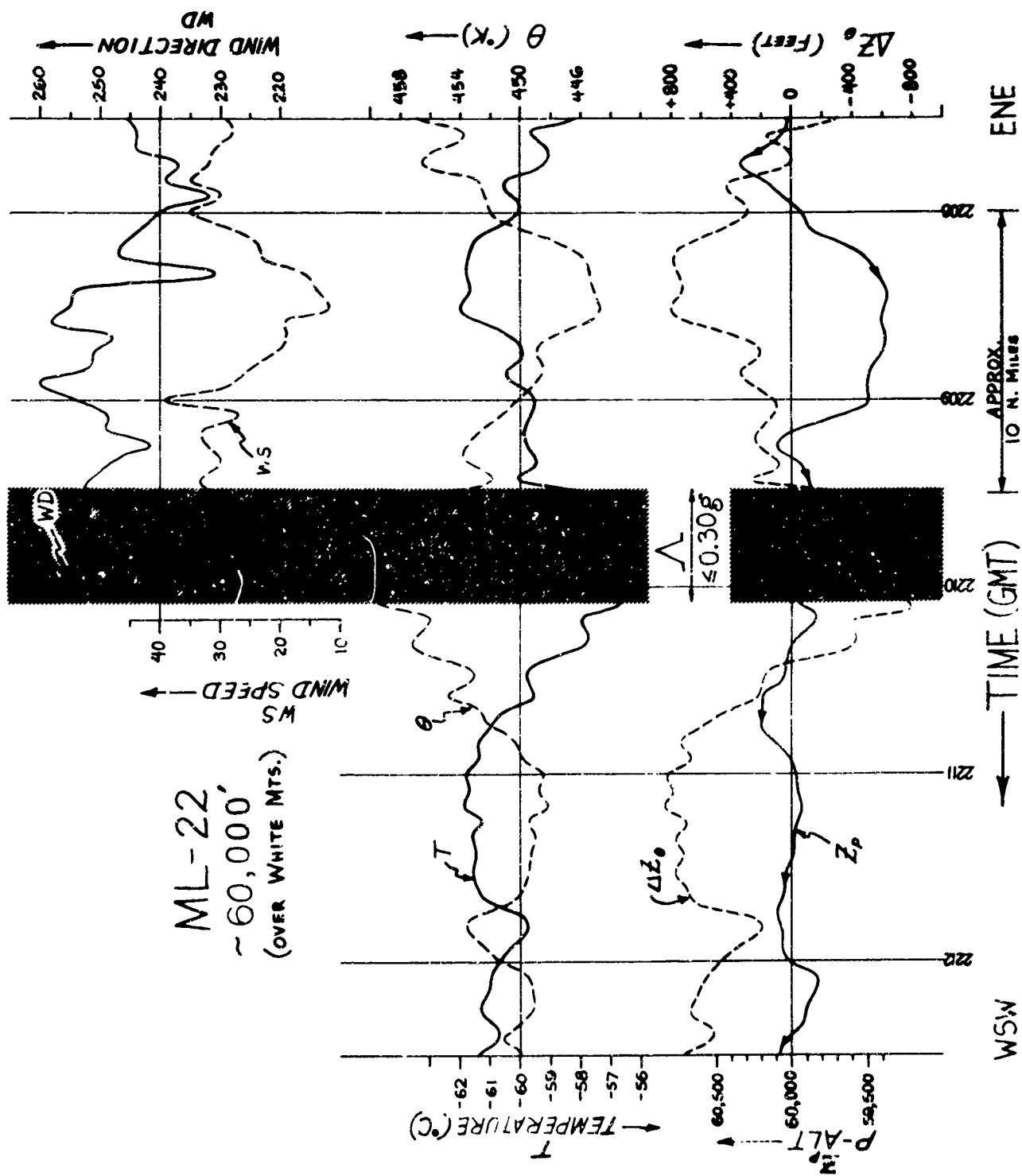(VICINITY OF MONO LAKE)

≤ 0.64 g

FIGURE 29.   Graphs of U-2 data for a portion of ML-22 traverse 1,

from 5-second data.

ML-22 ~60,000' (over White Mts.)

DOCUMENT CONTROL DATA - R & D

(Security classification of title, body of abstract and indexing annotation must be entered when the overall report is classified)

1. ORIGINATING ACTIVITY (Corporate author)	2a. REPORT SECURITY CLASSIFICATION
University of California Department of Meteorology Los Angeles, California 90024	Unclassified
	2b. GROUP

3. REPORT TITLE

OBSERVATIONS OF STRATOSPHERIC CLEAR-AIR TURBULENCE AND
MOUNTAIN WAVES OVER THE SIERRA NEVADA MOUNTAINS

4. DESCRIPTIVE NOTES (Type of report and inclusive dates)
Scientific. Final. 14 June 1964 - 14 Sept. 1966 Approved 1/16/68

5. AUTHOR(S) (First name, middle initial, last name)

Roger A. Helvey

6. REPORT DATE	7a. TOTAL NO OF PAGES	7b. NO OF REFS
December 1967	59	none
8a. CONTRACT OR GRANT NO AF 19(628)-4146	9a. ORIGINATOR'S REPORT NUMBER(S) None
b. PROJECT, TASK, AND WORK UNIT NO. 8604-02-01	
c. DOD ELEMENT 61410014	9b. OTHER REPORT NO(S) (Any other numbers that may be assigned this report) AFCRL-68-0001
d. DOD SUBELEMENT 6806-804A-8604	

10. DISTRIBUTION STATEMENT

1 - Distribution of this document is unlimited. It may be released to the
Clearinghouse, Department of Commerce, for sale to the general public.

| 11. SUPPLEMENTARY NOTES

TECH, OTHER | 12. SPONSORING MILITARY ACTIVITY
Air Force Cambridge Research
Laboratories (CRH)
L. G. Hanscomb Field
Bedford, Massachusetts 01730 |

13. ABSTRACT

Data obtained from a specially-instrumented U-2 aircraft have been
used to relate clear-air turbulence with mountain wave structure, observed
during two research flights in the stratosphere over the Sierra Nevada Mountains
on 13 and 14 May, 1964. The several cases of severe turbulence encountered
took place in regions immediately downstream of wave troughs, in area of
decreased statis stability and slower wind speeds associated with the prevailing
upwind tilt of the waves. An expression for the Richardson number is obtained
which incorporates modifications imposed upon flow through stationary
disturbances such as mountain waves.

DD FORM 1 NOV 1473

14 KEY WORDS	LINK A		LINK B		LINK C	
	ROLE	WT	ROLE	WT	ROLE	WT
Turbulence						
High altitude						
Clear-air						
U-2 flights						
Mountain waves						
Sierra Nevada						